

# Thermochemical Property, Pathway and Kinetic Analysis on the Reactions of Allylic Isobutenyl Radical with O<sub>2</sub>: an Elementary Reaction Mechanism for Isobutene Oxidation

Chiung-Ju Chen and Joseph W. Bozzelli\*

Department of Chemical Engineering, Chemistry and Environmental Science, New Jersey Institute of Technology, Newark, New Jersey 07102

Received: March 20, 2000; In Final Form: August 11, 2000

Kinetics for the reactions of allylic isobutenyl radical (C=C(C)C) with molecular oxygen are analyzed by using quantum Rice–Ramsperger–Kassel (QRRK) theory for  $k(E)$  and master equation analysis for falloff. Thermochemical properties and reaction path parameters are determined by ab initio–Møller–Plesset (MP2-(full)/6-31g(d) and MP4(full)/6-31g(d,p)/MP2(full)/6-31g(d)), complete basis set model chemistry (CBS-4 and CBS-q with MP2(full)/6-31g(d) and B3LYP/6-31g(d) optimized geometries), and density functional (B3LYP/6-31g(d) and B3LYP/6-311+g(3df,2p)/B3LYP/6-31g(d)) calculations. An elementary reaction mechanism is constructed to model the experimental system, isobutene oxidation. The forward and reverse rate constants for initiation reaction  $C_2C=C + O_2 \leftrightarrow C=C(C)C + HO_2$  are determined to be  $1.86 \times 10^9 T^{1.301} \exp(-40939 \text{ cal}/RT)$  ( $\text{cm}^3 \text{ mol}^{-1} \text{ s}^{-1}$ ) and  $6.39 \times 10^8 T^{0.944} \exp(-123.14 \text{ cal}/RT)$  ( $\text{cm}^3 \text{ mol}^{-1} \text{ s}^{-1}$ ), respectively. Calculations on 2,5-dimethylhexa-1,5-diene, methacrolein, isobutene oxides, and acetone product formation from reaction of isobutene oxidation mechanism are compared with experimental data. Reaction of allylic isobutenyl radical + O<sub>2</sub> forms an energized peroxy adduct [C=C(C)COO•]\* with a shallow well (ca. 21 kcal/mol), which predominantly dissociates back to reactants. The reaction channels of the C=C(C)-COO•\* adduct include reverse reaction to reactants, stabilization to C=C(C)COO• radical, O–O bond fission to C=C(C)CO• + O, isomerization via hydrogen shift with subsequent  $\beta$ -scission or R•O–OH bond cleavage. The C=C(C)COO•\* adduct can also cyclize to four- or five-member cyclic peroxide-alkyl radicals. All the product formation pathways of allylic isobutenyl radical with O<sub>2</sub> involve barriers that are above the energy of the initial reactants. This results in formation of isomers that exist in steady state concentration at early time in oxidation, at low to moderate temperatures. The primary reaction is reverse dissociation back to reactants, with slower reactions from the distributed isomers to new products. The concentration of allylic isobutenyl radical accumulates to relatively high levels and the radical is consumed mainly through radical–radical processes in moderate temperature isobutene oxidation. Reactions of C=C(C)COO• cyclization to four or five-member cyclic peroxides require relative high barriers due to the near complete loss of  $\pi$  bond energy for the terminal double bond's twist needed in the transition states. These barriers are calculated as 28.02 (24.95) and 29.72 (27.98) kcal/mol at CBS-q/MP2(full)/6-31g(d) level with A factors of  $2.42 \times 10^{10}$  ( $3.28 \times 10^{10}$ ) and  $3.88 \times 10^{10}$  ( $6.09 \times 10^{10}$ ) s<sup>-1</sup> at 743 K, respectively, for four- and five-member ring cyclization. Data in parentheses are calculation at B3LYP/6-311+g(3df,2p)/B3LYP/6-31g(d). A new reaction path is proposed: C=C(C•)COOH  $\leftrightarrow$  C=C(C•)CO• + OH  $\leftrightarrow$  C=Y(CCOC) + OH, which is responsible for methylene oxirane formation (Y = cyclic). The reaction barrier for the C=C(C•)COOH reaction to C=C(C•)CO• + OH is evaluated as 42.45 (41.90) kcal/mol with an A factor of  $4 \times 10^{15}$  s<sup>-1</sup>. The reaction barrier of C=C(C•)COOH  $\rightarrow$  TS5  $\rightarrow$  C=Y(CCOC) + OH is calculated as 42.14 kcal/mol with an A factor of  $6.95 \times 10^{11}$  s<sup>-1</sup> at 743 K.

## Introduction

Alkenes are major initial products from pyrolysis, oxidation or photochemical reaction of alkanes. The double bond in alkenes allows both addition and abstraction reactions to occur which enhance complexity in studies on these compounds. The relatively high octane ratings for olefin blending suggest olefin reactions play an important role in pre-ignition chemistry related to engine knock. It is of value to try and understand the fundamental chemical pathways and reaction kinetics of olefin oxidation in this moderate to low-temperature combustion chemistry for future model development and optimization. The

oxidation reactions of olefins are also important in the atmosphere photochemistry of hydrocarbons, biochemical synthesis and metabolism.<sup>1–5</sup>

Brezinsky and Dryer<sup>6</sup> have studied the oxidation of isobutene and isobutene/*n*-octane mixture in a high temperature flow reactor. They attributed the inhibiting effect of isobutene on the progress of the *n*-octane oxidation to abstraction reactions of radicals with the isobutene which result in relatively unreactive isobutenyl radical and species, such as HO<sub>2</sub>, CH<sub>3</sub>, C=CC etc.

Ingham et al.<sup>7</sup> studied the oxidation of isobutene at temperature from 673 to 793 K and pressure at 60 Torr, in flow reactor (aged boric-acid-coated vessels), with slow flow, up to several

\* To whom correspondence should be addressed. E-mail: bozzelli@tesla.njit.edu.

minute reaction times. They report a rate constant for initiation reaction isobutene ( $C=C(C)C$ ) +  $O_2 \leftrightarrow$  allylic isobutenyl radical ( $C\dot{C}C(C)\dot{C}C$ ) +  $HO_2$  to be  $4.79 \times 10^{12} \exp(-38564.6 \text{ cal}/RT) \text{ cm}^3 \text{ mol}^{-1} \text{ s}^{-1}$ . They also report concentration profiles for selected reaction products 2,5-dimethylhexa-1,5-diene, methacrolein, isobutene oxide and acetone. Recently, Bauge et al.<sup>8</sup> have determined the global reactivity of isobutene ignition delays in shock-tube (at temperature from 1230 to 1930 K and pressure from 9.5 to 10.5 atm). They also measured the product profiles in the perfectly stirred reactor (at temperature from 833 to 913 K and 1 atm). They proposed a mechanism, which does not include the reactions of oxygen addition with  $C\dot{C}C(C)\dot{C}C$ , to model the product profiles measured from stirred reactor.

In this study, we perform a thermochemical and kinetic pathway analysis on the reactions of allylic isobutenyl radical ( $C\dot{C}C(C)\dot{C}C$ ) with oxygen using thermodynamic properties ( $\Delta H_f^\circ$ ,  $S^\circ$ , and  $C_p(300)$  to  $C_p(1500)$ ) derived by ab initio and density functional calculations. We utilize a chemical activation kinetic treatment incorporating quantum Rice–Ramsperger–Kassel (QRRK) theory for  $k(E)$  and master equation<sup>9a–d</sup> of Gilbert et al. for falloff on the energized adduct. A multichannel unimolecular Quantum RRK analysis is used for analysis of the stabilized adduct dissociations. Calculations for production of 2,5-dimethylhexa-1,5-diene, methacrolein, isobutene oxides and acetone from isobutene oxidation mechanism are compared to experimental data of Ingham et al.<sup>7</sup> Calculated reaction rates  $C\dot{C}C(C)\dot{C}C + O_2$  are in agreement with the experimental value of Knyazev et al.<sup>10</sup>

## Method

**Ab Initio and Density Functional Calculations.** The geometries of reactants, important intermediates, transition states and products in  $C\dot{C}C(C)\dot{C}C + O_2$  reaction system are pre-optimized using UHF/PM3 MOPAC<sup>11</sup> program, followed by optimizations and frequency calculations at MP2(full)/6-31g(d) and B3LYP/6-31g(d) levels of theory using the Gaussian 94<sup>12</sup> program. Transition state (TS) geometries are identified by the existence of only one imaginary frequency in the normal mode coordinate analysis, evaluation of the TS geometry, and the reaction coordinate's vibrational motion. Intrinsic reaction coordinate (IRC) calculations were performed for all MP2 calculated transition states to verify the reaction path.

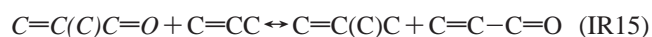
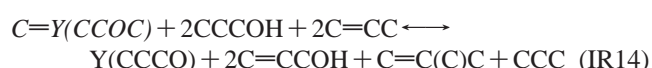
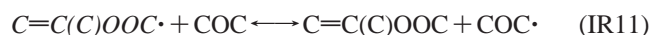
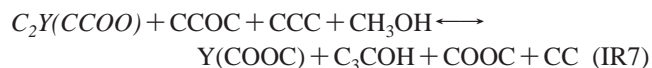
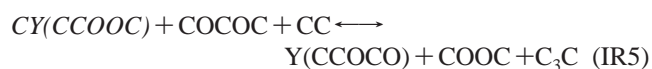
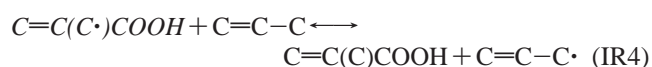
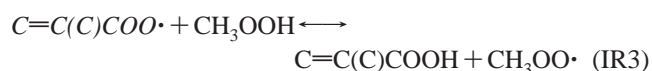
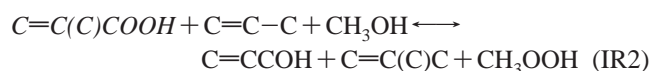
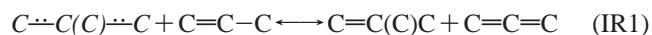
Complete basis set (CBS-4 and CBS-q) model chemistry calculations<sup>13–16</sup> are further performed in this study on the MP2(full)/6-31g(d) and B3LYP/6-31g(d) determined geometries. The CBS-q calculations include an SCF energy at HF/6-311+g(3df,2df,p), higher order correlation at QCISD(T)/6-31g, MP4(SDQ)/6-31g(d'), and second order correlation at MP2/6-31+g(d',p'). The 6-31g(d') and 6-31+g(d',p') are basis sets selected by the Petersson group.<sup>17,18</sup> CBS-q calculations are chosen because Jungkamp et al.,<sup>79,82</sup> Petersson et al.,<sup>84</sup> and our group<sup>19</sup> have shown that they result in reasonably accurate thermodynamic enthalpy data for these (5 or 6 heavy atoms) oxyhydrocarbon molecular systems. CBS-q and G2(MP2) are probably the best composite methods for these 6 heavy atoms systems.

**Thermodynamic Properties –  $\Delta H_f^\circ$ ,  $S^\circ$ , and  $C_p(300)$  to  $C_p(1500)$ .** Entropies and heat capacities are calculated based on frequencies and moments of inertia of the optimized MP2 (full)/6-31g(d) and B3LYP/6-31g(d) structures. Vibrational frequency contributions to entropies and heat capacities are scaled by 1.0228 and 1.0015 for MP2 (full)/6-31g(d) and B3LYP/6-31g(d) calculations, respectively, as recommended by Scott et al.<sup>20</sup> The method of Pitzer and Gwinn<sup>21</sup> is used for

thermodynamic analysis of  $S^\circ$ , and  $C_p(T)$  contribution from hindered internal rotors. The numbers of optical isomers and spin degeneracy of unpaired electrons are incorporated.

Zero-point vibrational energies (ZPVE) and thermal contributions to enthalpy are calculated at MP2 (full)/6-31g(d) and B3LYP/6-31g(d) levels. The vibrational frequency contributions to ZPVE are also scaled by 0.9661 and 0.9806 for MP2 (full)/6-31g(d) and B3LYP/6-31g(d) calculations, respectively. Total energies are calculated at MP2 (full)/6-31g(d), MP4 (full)/6-31g(d,p)//MP2 (full)/6-31g(d), B3LYP/6-31g(d), B3LYP/6-311+g(3df,2p)//B3LYP/6-31g(d) and complete basis set (CBS-4 and CBS-q) model chemistry calculations<sup>13–16</sup> and are available in the Supporting Information. The CBS-4 and CBS-q calculations are performed using geometry optimizations at MP2(full)/6-31g(d) and B3LYP/6-31g(d) levels of theory. Total energies (at 298 K) differences between TS and reactants, intermediates, and products determined at different theory levels are listed in Table 1.

Reactions (IR1–IR15) are used to determine  $\Delta H_f^\circ$  for reactant ( $C\dot{C}C(C)\dot{C}C$ ), intermediate radicals ( $C=C(C)COO\cdot$ ,  $C=C(C)\cdot COOH$ ,  $CY(C\cdot COOC)$ ,  $C_2\cdot Y(CCOO)$ ,  $C(YC_2O)CO\cdot$ ,  $C=C(C)OOC\cdot$  and  $C\cdot OOH$ ) and products ( $C=Y(CCO)$  and  $C=C(C)C=O$ ) in the reaction systems of this study (target species). These reactions conserve both bond types (isodesmic) and groups. Calculations are performed on each species in the reaction to determine  $\Delta H_{rxn,298}$ .  $\Delta H_f^\circ$  values of the needed species in a reaction are determined from the  $\Delta H_{rxn,298}$  and evaluated literature  $\Delta H_f^\circ$  values of the remaining species.



(target species are italicized)

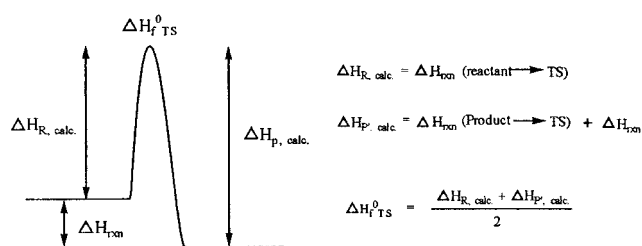
TABLE 1: Total Energy (at 298 K) Differences between TSs and Reactants, Intermediates and Products<sup>a</sup> (in kcal/mol)

	CBS-4		CBS-q		MP2(full) <sup>b</sup>		MP4(full) <sup>c</sup>		CBS-4		CBS-q		B3LYP <sup>b</sup>		B3LYP311 <sup>d</sup>	
	G3MP2	//MP2(full)/6-31g(d)						//B3LYP/6-31g(d)								
C=C(C)C+O <sub>2</sub> ⇒ ts1	-0.89	-4.78	1.47	18.21 (4.70) <sup>e</sup>	13.98 (-1.89) <sup>f</sup>	-6.0	12.22	-1.39	-0.01							
C=C(C)COO• ⇒ ts1	20.77	11.30	21.51	32.72 (7.87) <sup>e</sup>	30.56 (7.56) <sup>f</sup>	11.42	34.59	15.41	15.16							
C=C(C)COO• ⇒ ts2		37.62	38.86	48.69	46.56	38.30	37.81	39.99	37.81							
C=C(C)COO• ⇒ ts3	24.81	21.54	22.39	30.61	28.84	20.90	23.55	23.69	21.54							
C=C(C•)CQ ⇒ ts3	21.88	21.82	18.88	24.77	22.87	18.98	16.97	14.64	17.55							
C=C(C•)CQ ⇒ ts4		51.59	48.52	63.94	61.41	50.98	47.57	50.65	47.92							
C=C=C+C•OOH ⇒ ts4		3.93	4.21	19.35	17.34	3.63	3.40	7.67	10.02							
C=C(C•)CQ ⇒ ts5		42.26	39.11	52.88	47.80	40.79	38.10	31.79	30.38							
C=Y(CCOC)+OH ⇒ ts5		47.55	44.10	60.34	55.14	45.93	42.94	30.21	31.87							
C=C(C•)CQ ⇒ ts14		56.36	54.12	58.64	57.56	52.99	50.13	53.03	52.09							
C=C(C)COO• ⇒ ts6		28.15	29.53	36.25	34.50	28.53	30.67	28.43	29.20							
C2•Y(CCOC) ⇒ ts6		10.37	11.50	27.66	16.55	11.99	10.77	7.59	6.97							
C2•Y(CCOC) ⇒ ts7		14.76	17.20	32.65	23.80	19.43	17.81	15.06	13.90							
C=C(C)OOC• ⇒ ts7		20.65	21.49	31.43	29.43	21.02	20.11	19.29	21.05							
C2•Y(CCOC) ⇒ ts8		12.66	17.55	37.64	22.92	18.63	19.48	12.05	11.77							
CCY(CCOC)CO• ⇒ ts8						66.41	65.72	58.16	59.36							
C=C(C)COO• ⇒ ts9		27.05	28.84	35.22	33.13	27.60	30.26	26.45	26.72							
CY(C•CCOO) ⇒ ts9		27.48	25.89	40.86	34.87	26.47	24.88	23.42	21.95							
C=C(C)C+O <sub>2</sub> ⇒ ts10		48.20	40.88	64.99		46.53	39.93	37.37	34.80							
C=C(C)C+HO <sub>2</sub> ⇒ ts10		2.33	0.28	3.27		-0.33	-0.92	-5.09	-1.75							
CY(C•CCOO) ⇒ ts11						21.54	14.87	18.07	11.99							
CCY(C2O)CO• ⇒ ts11						53.91	46.59	46.39	42.12							

<sup>a</sup> Reaction enthalpies include thermal correction and zero-point energy correction. <sup>b</sup> Based on 6-31g(d) basis set. <sup>c</sup> Based on 6-31g(d,p) basis set. <sup>d</sup> B3LYP/6-311+g(3df,2p) level. <sup>e</sup> From PMP2(full)/6-31g(d). <sup>f</sup> From PMP4(full)/6-31g(d,p)//MP2(full)/6-31g(d).

Group balance reaction enthalpies (IR1–IR15) are calculated at CBS-q//MP2(full)/6-31g(d), CBS-q//B3LYP/6-31g(d), MP4(full)/6-31g(d,p)//MP2(full)/6-31g(d), MP2(full)/6-31g(d), B3LYP/6-311+g(3df,2p)//B3LYP/6-31g(d), and B3LYP/6-31g(d) levels and listed in Table 2.  $\Delta H_f^{\circ}$  of reactant, intermediate radicals and products calculated from group balance isodesmic reactions at various levels listed in Table 3. We note that value accurate to 1 digit after the decimal for the kcal/mol units.

#### $\Delta H_f^{\circ}$ TS Reaction Scheme



Calculation of enthalpy of formation for transition states is NOT taken as the total energy difference between reactant(s) and transition state but is illustrated in the  $\Delta H_f^{\circ}$  TS Reaction Scheme above.  $\Delta H_f^{\circ}$  TS is calculated by an average of two values  $\Delta H_{R, \text{calc.}}$  and  $\Delta H_{P, \text{calc.}}$ .  $\Delta H_f^{\circ}$  of products and reactants are first obtained from group balance isodesmic reactions (IR1–IR15).  $\Delta H_{R, \text{calc.}}$  is the difference between the calculated energy of the TS and reactant(s).  $\Delta H_{P, \text{calc.}}$  is the difference between the calculated energy of the TS and product(s) plus  $\Delta H_{\text{rxn}}$  ( $\Delta H_f^{\circ} \text{product(s)} - \Delta H_f^{\circ} \text{reactant(s)}$ ). Thermodynamic parameters –  $\Delta H_f^{\circ}$ ,  $S^{\circ}$ , and Cp(300) to Cp(1500) for species in C=C(C)C + O<sub>2</sub> reaction system are listed in Table 4.

**Kinetic Calculations.** Unimolecular dissociation and isomerization reactions of the chemically activated and stabilized adducts resulting from addition or combination reactions are analyzed by first constructing potential energy diagrams for the reaction system. Thermodynamic parameters,  $\Delta H_f^{\circ}$ ,  $S^{\circ}$ , Cp(T), reduced vibration frequency sets, and Lennard Jones parameters for species in each reaction path are presented.

High-pressure rate constants ( $k_{\infty}$ ) for each channel are obtained from ab initio calculation, literature, or referenced estimation techniques. Kinetics parameters for unimolecular and bimolecular (chemical activation) reactions are then calculated using multi-frequency QRRK analysis for  $k(E)^{22-24}$  with the steady-state assumption on the energized adduct(s). The master equation analysis<sup>9a-d</sup> as discussed by Gilbert is used for falloff. ( $\Delta E^{\circ}_{\text{down}}$  of 1000 cal/mol<sup>88,89</sup> is used for master equation analysis, N<sub>2</sub> is the third body.

Reactions that incur a change in number of moles, such as unimolecular dissociation, have energy of activation calculated as  $\Delta U_{\text{rxn}}$  plus an  $E_a$  for the reverse addition, where  $U$  is internal energy ( $E_a$  reverse is usually 0.0 for simple association reactions).

#### Input Information Requirements for QRRK Calculation.

Preexponential factors ( $A_{\infty}$ s) are calculated using canonical TST<sup>25</sup> along with MP2 or DFT-determined entropies of intermediates and TSs for the reactions where thermodynamic properties of TS are available. High-pressure rate constants ( $k_{\infty}$ ) are represented using three parameters  $A$ ,  $n$  and  $E_a$  over a temperature range of 300 to 2000 K as expressed below.

$$k_{\infty} = A(T)^n \exp(-E_a/RT)$$

High-pressure limit preexponential factors for combination reactions are obtained from the literature and from trends in homologous series of reactions.

Reduced sets of three vibration frequencies and their associated degeneracies are computed from fits to heat capacity data, as described by Ritter<sup>26</sup> and Bozzelli et al.<sup>27</sup> These have been shown by Ritter to accurately reproduce molecular heat capacities, Cp(T), and by Bozzelli et al.<sup>27</sup> to yield accurate ratios of density of states to partition coefficient,  $\rho(E)/Q$ .

Lennard–Jones parameters, sigma (Angstroms) and  $\epsilon/k$  (Kelvins), are obtained from tabulations<sup>28</sup> and from a calculation method based on molar volumes and compressibility.<sup>29</sup> When necessary, estimation is done in a consistent and uniform manner via use of generic reaction rate constants with reference to

**TABLE 2: Group Balance Reaction Enthalpies (in kcal/mol)**

reactions	CBS-4	CBS-q	MP2(full) <sup>a</sup>	MP4(full) <sup>b</sup>	CBS-4	CBS-q	B3LYP <sup>a</sup>	B3LYP311 <sup>c</sup>
	//MP2(full)/6-31g(d)				//B3LYP/6-31g(d)			
C=C(C)C + C=CC ⇌ C=C(C)C + C=C=C	-1.38	-1.40	-2.08	-1.75	-1.45	-1.46	-1.72	-1.65
C=C(C)COOH + C=CC + CH3OH ⇌ C=CCOH + C=C(C)C + CH3OOH	0.59	0.72	0.73	0.72	2.27	2.45	0.89	0.06
C=C(C)COO· + CH3OOH ⇌ C=C(C)COOH + CH3OO·	-1.22	-1.06	-2.27	-2.19	-0.44	0.28	-0.42	-0.14
C=C(C)COOH + C=CC ⇌ C=C(C)COOH + C=C=C	-0.61	-0.74	-0.87	-0.37	-2.26	-2.40	-1.12	-1.29
CY(CCOOC) + COOC + CC ⇌ Y(CCOCO) + COOC + C3C	3.14	3.63	3.19	3.57	2.37	2.89	2.26	1.57
CY(CCOOC) + CC· ⇌ CY(C·COOC) + CC	-2.30	-2.53	-2.50	-2.87	-2.99	-3.24	-6.08	-5.17
C2Y(CCOO) + CCOC + CCC + COH ⇌ Y(CCCO) + C3COH + COOC + CC	-1.30	-0.22	-0.08	0.75	-1.72	-0.77	-0.86	-0.75
C2Y(CCOO) + CC· ⇌ C2·Y(CCOO) + CC	6.79	0.36	1.34	6.77	-0.07	-0.91	0.31	0.80
C·OOH + CH3OH ⇌ COOH + C·OH	-2.43	-2.13	-3.12	-2.87	-2.21	-1.93	-1.75	-1.54
C=C(C)OOC + COOH ⇌ COOC + C=C(C)OOH	0.83	1.03	0.50	0.64	0.32	0.51	-0.57	-0.70
C=C(C)OOC + COC· ⇌ C=C(C)OOC· + COC	2.14	2.01	2.64	2.58	3.14	2.79	2.87	3.06
CY(C2O)COH + CC ⇌ Y(CCO) + C3COH	3.44	3.60	4.47	4.73	3.43	3.54	5.92	3.48
CY(C2O)COH + CH3O· ⇌ CY(C2O)CO· + CH3OH					4.11	3.99	3.06	1.67
C=CY(CCOOC) + 2 CCOH + 2C=CC ⇌ Y(CCCO) + 2C=CCOH + C=C(C)C + CCC	2.97	3.59	1.00	1.55	3.21	3.81	2.53	1.04
C=C(C)C=O + C=CC ⇌ C=C(C)C + C=CC=O	1.26	1.22	1.31	1.27	1.19	1.24	1.09	0.95

**TABLE 3: Enthalpies (at 298 K) of Reactant, Intermediates, and Products Calculated from Isodesmic Reactions (IR1–IR15)<sup>d</sup>**

reactions	CBS-4	CBS-q	MP2(full) <sup>a</sup>	MP4(full) <sup>b</sup>	CBS-4	CBS-q	B3LYP <sup>a</sup>	B3LYP311 <sup>c</sup>
	//MP2(full)/6-31g(d)				//B3LYP/6-31g(d)			
C=C(C)C	32.54	32.56	33.24	32.91	32.61	32.62	32.88	32.81
C=C(C)COOH	-24.38	-24.51	-24.52	-24.51	-26.06	-26.24	-24.68	-23.85
C=C(C)COO·	11.34	11.06	12.25	12.18	8.88	7.98	10.24	10.79
C=C(C)COOH	11.19	11.19	11.30	10.82	11.16	11.12	11.40	12.40
CY(CCOOC)	-33.82	-34.31	-33.87	-34.25	-33.05	-33.57	-32.94	-32.25
CY(C·COOC)	13.39	12.66	13.12	12.37	13.46	12.68	10.48	12.07
C2Y(CCOO)	-19.06	-20.14	-20.28	-21.11	-18.64	-19.59	-19.50	-19.61
C2·Y(CCOO)	37.23	29.73	30.56	35.16	30.79	29.01	30.31	30.69
C·OOH	15.03	14.73	15.72	15.47	14.81	14.53	14.35	14.14
C=C(C)OOC	-19.94	-20.14	-19.61	-19.75	-19.43	-19.62	-18.54	-18.41
C=C(C)OOC·	26.79	26.46	27.63	27.42	28.29	27.76	28.92	29.24
CY(C2O)COH	-70.17	-70.33	-71.20	-71.46	-70.16	-70.27	-72.65	-70.21
CY(C2O)CO·					-13.98	-14.20	-17.51	-16.46
C=CY(CCOOC)	1.64	1.02	3.61	3.06	1.40	0.80	2.08	3.57
C=C(C)C=O	-28.39	-28.35	-28.44	-28.40	-28.32	-28.37	-28.22	-28.08

<sup>a</sup> Based on 6-31g(d) basis set. <sup>b</sup> Based on 6-31g(d,p) basis set. <sup>c</sup> B3LYP/6-311+g(3df,2p) level <sup>d</sup> Literature data used in isodesmic reaction to determine  $\Delta H_{298}^\circ$  of species studied in this work:  $\Delta H_{298}^\circ$  of (CC) = -20.54 (ref 43); (C3C) = -32.27 (ref 44); (C=CC) = 4.71 (ref 44); (C=C(C)C) = -3.8 (ref 43); (C=CCOH) = -31.52 (ref 44); (C=C(C)OOH) = -19.91 (based on CBS-q//B3LYP/6-31g(d) calculation); (C3COH) = -74.69 (ref 45); (COOH) = -31.8 (ref 46); (CCCOH) = -67.85 (ref 43); (COOC) = -31.00 (ref 46); (CCOC) = -51.74 (ref 45); (COCOC) = -83.27 (ref 45); (CC=CC=O) = -18.61 (Average value of ref 43, ref 44 and ref 49); (YCCO) = -12.58 (ref 47); (YCCCO) = -19.24 (ref 45); (YCCOCO) = -71.22 (ref 45); bond dissociation energy  $DH_{298}^\circ$  of (CC-H) = 101.6 (ref 48); (C=CC-H) = 87.06 (ref 48); (COO-H) = 86.6 (ref 46); (CH3O-H) = 104.8 (ref 46); H-CH2OH = 96.5 (ref 48); COC-H = 96.69 (ref 48 based on G2 and CBSQ calculations); in kcal/mol.

literature, experiment or theoretical calculation in each case. The QRRK calculation input parameters and their references are listed in the table associated with the respective reaction system. Also use of a representative manifold of frequencies plus incorporation of one external rotation for the density of states,  $\rho(E)/Q$  and in calculation of  $k(E)$ . The Leonard-Jones collision frequency  $Z_{LJ}$  is calculated by  $Z_{LJ} = Z\Omega$  (2,2) integral<sup>28,29</sup> obtained from fit of Reid et al.<sup>29</sup>

The QRRK analysis for  $k(E)$  with modified strong collision and a constant  $F_E$  for falloff has been used previously to analyze a variety of chemical activation reaction systems, Westmoreland et al.,<sup>22,23</sup> Dean et al.,<sup>24</sup> and Bozzelli et al.<sup>30,31</sup> There are a number of recent publications by other researchers that utilize the QRRK formalism with a more exact calculation  $F_E$  in modified strong collision analysis<sup>58-63</sup> or utilize just a QRRK formalism.<sup>64,65</sup> It is shown to yield reasonable results in these applications and provides a framework by which the effects of temperature and pressure can be evaluated for complex chemical

activation or unimolecular dissociation reaction systems. The QRRK formalism used in this work is recently described by Chang et al.<sup>56</sup> The C=C(C)C + O<sub>2</sub> reaction system in this study is complex; it includes 9 adducts, 10 transition states and 9 product sets. The QRRK analysis with either modified strong collision or master equation for falloff is a reasonable method to estimate the chemical activation rate constants to adducts and product sets as a function of temperature and pressure for all the channels in this complex system. We note that both forward and reverse paths are included for adducts; but product formation is not reversible in the analysis.

## Results and Discussion

**Formation of Allylic Isobutenyl Radical (C=C(C)C); Reaction Initiation.** There are two reaction initiation processes: abstraction of hydrogen by O<sub>2</sub> and unimolecular dissociation. The resonance stabilized C=C(C)C is formed by abstraction

TABLE 4: Thermodynamic Properties

species	$\Delta H_{f,298}^{\circ}$ (kcal/mol)	$S_{298}^{\circ}$ (cal/mol-K)	$Cp_{300}$ (cal/mol-K)	$Cp_{400}$	$Cp_{500}$	$Cp_{600}$	$Cp_{800}$	$Cp_{1000}$	$Cp_{1500}$
N2	0	45.7	6.65	6.86	6.99	7.1	7.31	7.61	7.98
O	59.52	38.4	5	5	5	5	5	5	5
O2	0	49	6.82	7.15	7.36	7.51	7.82	8.24	8.69
OH	9.5	43.8	6.79	6.86	6.93	7	7.14	7.28	7.61
CH2O	-26	50.92	8.48	9.49	10.51	11.51	13.33	14.82	16.98
Using THERM Group Additivity									
C*C*C	45.92	58.31	14.19	17.22	19.8	21.99	25.46	28.02	32.03
CC*C*O	-4.7	70.37	18.07	21.88	25.19	28.06	32.66	36.06	41.08
C2*C*O	-9.26	72.5	18.29	22.29	25.76	28.75	33.51	36.93	41.75
CCYC*CO	24.48	72.61	15.77	20.22	24.03	27.29	32.38	35.96	40.98
C*C(C)CO•	11.52	80.05	23.92	29.37	34.05	37.95	44.03	48.55	55.62
CC(CO•)CO	-35.04	90.22	25.71	31.8	37.01	41.44	48.37	53.35	60.64
CCYCC*OOC	9.02	77.14	23.78	31.27	37.4	42.41	49.81	54.82	62.17
C*C(C)C*Q	9.12	88.48	28.7	34.38	39.22	43.34	49.77	54.38	61.06
DIC2*C*C	3.28	104.51	40.98	51.42	60.39	68.07	80.26	89.21	102.88
Using CBS-q//MP2(full)//6-31G(d) Calculations									
C•H2OOH	14.73	68.26 <sup>a</sup>	16.57	18.39	19.95	21.27	23.36	24.86	27.04
C <sup>••</sup> C(C) <sup>••</sup> C	32.56	70.99 <sup>a</sup>	20.96	26.09	30.52	34.22	40.07	44.43	51.22
C*C(C)CQ•	11.06	89.72	25.26	30.42	35.17	39.27	45.8	50.78	58.76
C*C(C•)CQ	11.19	90.07	26.72	33.27	38.79	43.22	49.64	54.07	60.8
CCYC*COOC	12.66	78.38	23.71	30.14	35.9	40.73	48.11	53.42	61.47
C2•CYCCOO	29.73	79.36	25.03	31.53	37.13	41.71	48.54	53.40	60.87
C*CYCCOC	1.02	69.51	18.66	24.29	29.35	33.59	40.06	44.71	51.79
C*CICC*O	-28.22	75.91 <sup>a</sup>	21.55	26.46	30.84	34.59	40.51	44.84	51.3
C*CICOOOC•	26.46	95.07 <sup>a</sup>	29.09	34.87	39.37	43.28	50	54.82	
C=C(C•)CO•(singlet)	44.94	77.22 <sup>b</sup>	23.15	28.46	32.83	36.38	41.77	45.71	51.86
C=C(C•)CO•(triplet)	43.91	79.11 <sup>b</sup>	23.11	28.49	32.88	36.44	41.84	45.76	51.89
TS1	34.03	90.96	25.13	30.15	34.74	38.72	45.03	49.82	57.43
TS2	49.92	85.16	24.28	29.86	34.93	39.27	46.08	51.1	58.82
TS3	31.76	78.39	23.01	29.68	35.55	40.43	47.81	53.03	60.85
TS4	62.17	96.19	29.54	35.14	39.85	43.64	49.23	53.2	59.39
TS5	52.46	83.44	25.31	31.15	36.15	40.28	46.6	51.31	58.93
TS6	40.91	78.4	23.29	28.98	34.24	38.77	45.86	51.06	59.14
TS7	47.44	78.29	24.19	30.09	35.28	39.65	46.43	51.42	59.26
TS8	47.28	79.92	25.32	31.05	36.14	40.43	47.07	51.95	59.59
TS9	39.23	77.66	22.41	28.35	33.83	38.51	45.77	51.05	59.18
TS10	36.71	96.11	26.22	32.23	37.63	42.16	48.95	53.59	60.16
TS14	65.31	84.43	25.97	32.32	37.75	42.17	48.64	53.14	59.92
Using B3LYP/6-31G(3df,2p)//B3LYP/6-31G(d) Calculations									
C•H2OOH	14.14	68.26 <sup>a</sup>	16.57	18.39	19.95	21.27	23.36	24.86	27.04
C <sup>••</sup> C(C) <sup>••</sup> C	32.81	70.99 <sup>a</sup>	20.96	26.09	30.52	34.22	40.07	44.43	51.22
C*C(C)CQ•	10.79	90.11	25.99	31.41	36.34	40.56	47.19	52.12	59.76
C*C(C•)CQ	12.4	90.33	27.21	33.78	39.27	43.66	50.05	54.45	61.08
CCYC*COOC	12.07	79.44	24.18	30.71	36.5	41.35	48.72	53.99	61.91
C2•CYCCOO	30.69	79.60	25.45	32.09	37.73	42.30	49.09	53.91	61.25
C*CYCCOC	3.57	69.02	18.84	24.57	29.68	33.94	40.42	45.06	52.06
C*CICC*O	-28.08	75.91 <sup>a</sup>	21.55	26.46	30.84	34.59	40.51	44.84	51.3
CCY(C2O)CO•	-16.46	86.14 <sup>a</sup>	25.42	32.21	38.41	42.71	49.74	54.51	
C*CICOOOC•	29.24	95.07 <sup>a</sup>	29.09	34.87	39.37	43.28	50	54.82	
C=C(C•)CO•(singlet)	45.65	77.22	23.15	28.46	32.83	36.38	41.77	45.71	51.86
C=C(C•)CO•(triplet)	44.62	79.11	23.11	28.49	32.88	36.44	41.84	45.76	51.89
TS1	32.81	92.67	26.8	31.88	36.38	40.21	46.25	50.81	58.05
TS2	48.6	86.3	25.87	31.91	37.12	41.43	47.96	52.65	59.77
TS3	31.14	78.22	24.08	31.07	37.01	41.84	49	54	61.45
TS4	65.16	92.96	27.7	33.39	38.24	42.18	48	52.15	58.68
TS5	43.86	84.54	26.92	32.87	37.89	41.98	48.19	52.72	59.91
TS6	38.83	79.39	24.77	30.71	35.97	40.38	47.18	52.14	59.81
TS7	47.44	79.93	26.25	32.27	37.38	41.57	47.98	52.68	60.03
TS8	41.97	78.46	24.85	30.92	36.21	40.61	47.36	52.28	59.88
TS9	35.77	78.41	23.56	29.74	35.24	39.83	46.88	51.98	59.78
TS10	36.13	96.87	27.64	33.72	39.04	43.42	49.93	54.37	60.64
TS11	28.54	80.42	24.94	30.73	36.09	40.72	47.92	53.08	60.70
TS12	52.06	73.99	21.64	26.64	30.97	34.58	40.15	44.25	50.61
TS13	47.37	70.54	19.71	25.22	29.94	33.81	39.67	43.9	50.42
TS14	64.49	86.24	27.68	34.20	39.68	44.06	50.37	54.65	60.92

<sup>a</sup> *S* and *Cp*(*T*) from THERM.<sup>43</sup> <sup>b</sup> *S* and *Cp*(*T*) from B3LYP/6-31G(3df,2p)//B3LYP/6-31G(d) calculations.

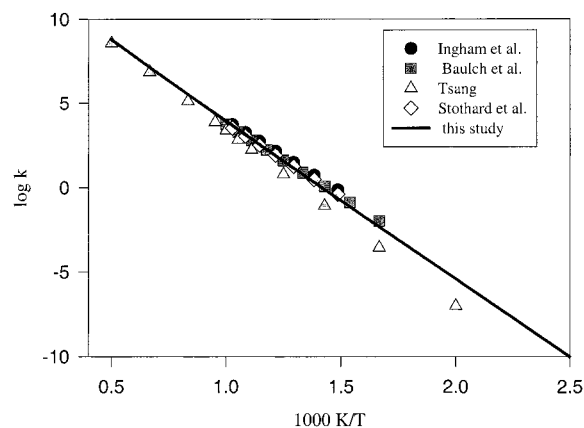
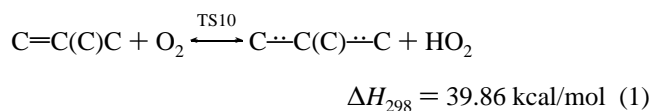


**Figure 1.** Comparison of the calculated rate constant of  $\text{C}_2\text{C}=\text{C} + \text{O}_2 \rightarrow \text{C}=\text{C}(\text{C})\text{C} + \text{HO}_2$  with experimental values for similar reaction of  $\text{C}=\text{C}-\text{C} + \text{O}_2 \rightarrow \text{C}=\text{C}-\text{C} + \text{HO}_2$ . Circles: Ingham et al.,<sup>7</sup>  $k(\text{C}_2\text{C}=\text{C} + \text{O}_2 \rightarrow \text{C}=\text{C}(\text{C})\text{C} + \text{HO}_2) = 4.79 \times 10^{12} \exp(-19388 \text{ K}/T) \text{ cm}^3 \text{ mol}^{-1} \text{ s}^{-1}$ ; squares: Baulch et al.,<sup>50</sup>  $k(\text{C}=\text{C}-\text{C} + \text{O}_2 \rightarrow \text{C}=\text{C}-\text{C} + \text{HO}_2) = 1.93 \times 10^{12} \exp(-19700 \text{ K}/T) \text{ cm}^3 \text{ mol}^{-1} \text{ s}^{-1}$ ; triangles: Tsang, W.,<sup>33</sup>  $k(\text{C}=\text{C}-\text{C} + \text{O}_2 \rightarrow \text{C}=\text{C}-\text{C} + \text{HO}_2) = 6.03 \times 10^{15} \exp(-23950 \text{ K}/T) \text{ cm}^3 \text{ mol}^{-1} \text{ s}^{-1}$ ; rhombuses: Stothard et al.,<sup>57</sup>  $k(\text{C}=\text{C}-\text{C} + \text{O}_2 \rightarrow \text{C}=\text{C}-\text{C} + \text{HO}_2) = 1.95 \times 10^{12} \exp(-19664 \text{ K}/T) \text{ cm}^3 \text{ mol}^{-1} \text{ s}^{-1}$ .

the weakly bonded hydrogen atom (the allylic C–H bond is 88.1 kcal/mol) from isobutene. The endothermic initiation reaction 1 is a key rate-determining reaction in moderate temperature isobutene oxidation.

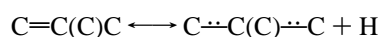


We find a small barrier of 0.28 kcal/mol based on CBS-q//MP2(full)/6-31g(d) calculation and no barrier based on B3LYP/6-311+g(3df,2p)//B3LYP/6-31g(d) calculation for reverse reaction 1.

Arrhenius preexponential factor,  $A_{\infty}$ , is calculated via canonical TST. The high-pressure limit rate constants, fit by a three parameter ( $A$ ,  $n$ ,  $E_a$ ) modified Arrhenius Equation over temperature range 300 K to 2000 K, are  $1.86 \times 10^9 T^{1.301} \exp(-40939 \text{ cal}/RT) \text{ cm}^3 \text{ mol}^{-1} \text{ s}^{-1}$  and  $6.39 \times 10^8 T^{0.944} \exp(-123.14 \text{ cal}/RT) \text{ cm}^3 \text{ mol}^{-1} \text{ s}^{-1}$  for forward and reverse reaction 1, respectively, based on CBS-q//MP2(full)/6-31g(d) calculation. Comparison of our calculated rate constant with experimental values for the similar reaction of allyl radical,  $\text{C}=\text{C}-\text{C} + \text{O}_2 \rightarrow \text{C}=\text{C}-\text{C} + \text{HO}_2$ , is shown in Figure 1. The agreement of our calculated rate constants with experimental values supports our methods for estimating kinetic parameters.

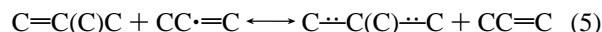
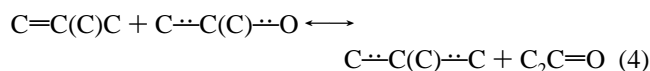
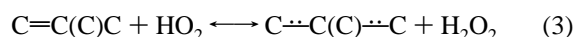
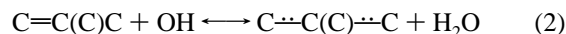
Sensitivity analysis shows that in reaction mechanism an increase in the A factor of reaction 1 by a factor of 2, results in an increase of acetone, methacrolein, 2,5-dimethylhexa-1,5-diene, and methylene oxirane formations by 6.48% (6.8%), 7.39% (7.86%), 6.82% (7.84%), and 10.70% (11.90%), respectively, at 743 K and 60 Torr (reaction time = 180 s). Results are based on thermodynamic properties calculated from CBS-q//MP2(full)/6-31g(d), data in parentheses are from B3LYP/6-311+g(3df,2p)//B3LYP/6-31g(d) calculation.

The unimolecular decomposition of isobutene to allylic isobutenyl radical with H atom is also included in mechanism.



We use high-pressure limit rate constant  $2 \times 10^{15} \exp(-87390 \text{ cal}/RT) \text{ (s}^{-1}\text{)}$  obtained from experimental data of Douhou et al.<sup>32</sup>

The radicals, OH, HO<sub>2</sub> and CH<sub>3</sub>COCH<sub>2</sub>• ( $\text{C}=\text{C}(\text{C})\text{C}\text{O}\cdot$ ), can undergo abstraction reaction 2, 3, and 4 to form allylic isobutenyl radical under moderate temperature oxidation condition, with CH<sub>3</sub>C•CH<sub>2</sub> ( $\text{C}-\text{C}=\text{C}$ ) having less importance.

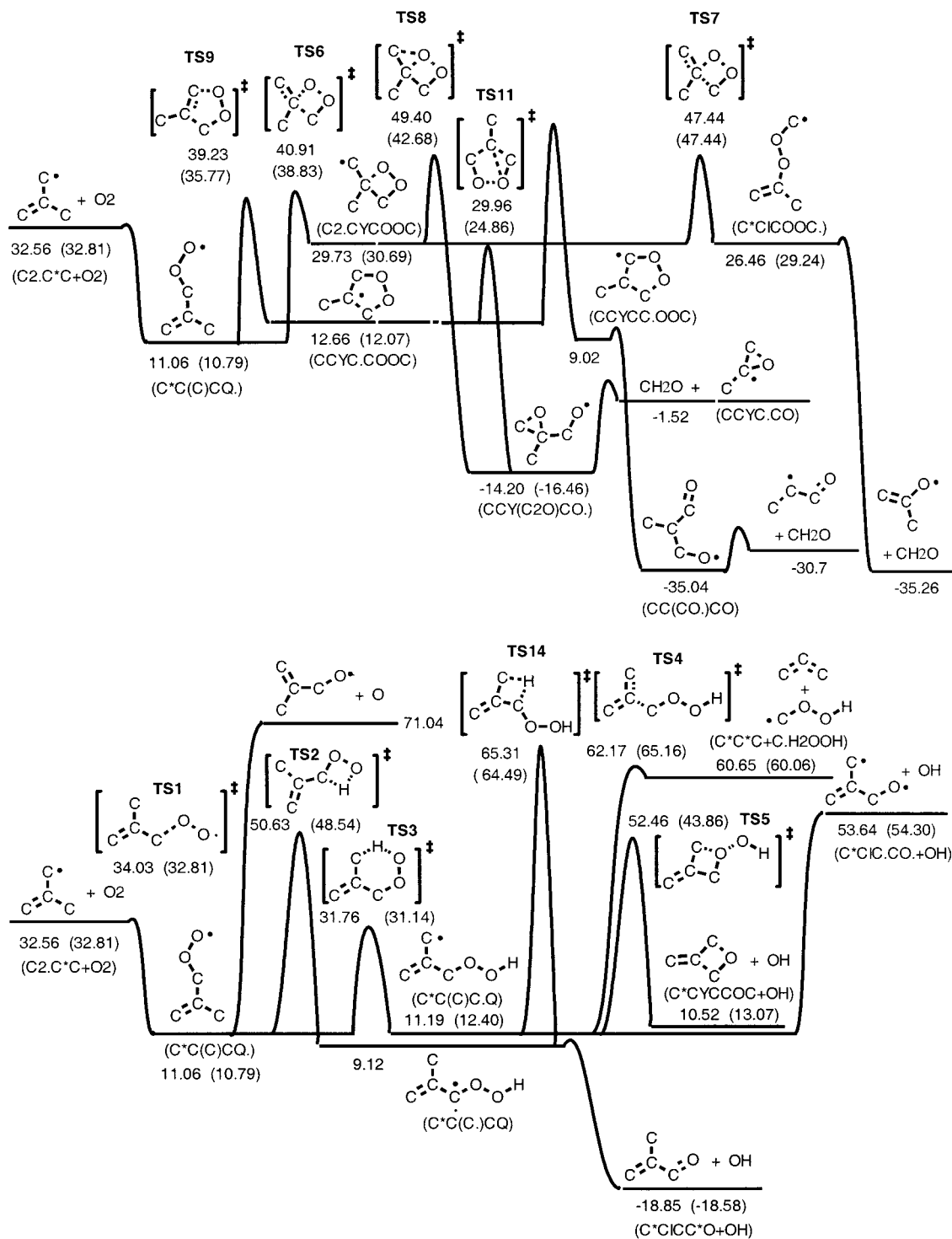


We use rate constants  $4.68 \times 10^6 T^{2.0} \exp(298 \text{ cal}/RT) \text{ (cm}^3 \text{ mol}^{-1} \text{ s}^{-1}\text{)}$  and  $1.93 \times 10^4 T^{2.6} \exp(-13910 \text{ cal}/RT) \text{ (cm}^3 \text{ mol}^{-1} \text{ s}^{-1}\text{)}$  for reaction 2 and 3, respectively, following the analogous reaction of propene<sup>33</sup> and adjustment for steric effects. Rate constants of reaction 4 and 5 are  $2.23 \times T^{3.5} \exp(-6637 \text{ cal}/RT) \text{ (cm}^3 \text{ mol}^{-1} \text{ s}^{-1}\text{)}$  and  $4.42 \times T^{3.5} \exp(-4682 \text{ cal}/RT) \text{ (cm}^3 \text{ mol}^{-1} \text{ s}^{-1}\text{)}$ . The radical  $\text{C}-\text{C}=\text{C}$  arises from  $\beta$ -scission of  $\text{C}=\text{C}(\text{C})\text{CO}\cdot$ , which is formed from cleavage of the weak (ca. 43 kcal/mol) O–O single bond of  $\text{C}=\text{C}(\text{C})\text{COOH}$ . The  $\text{C}=\text{C}(\text{C})\text{CO}\cdot$  undergoes  $\beta$ -scission forming  $\text{C}-\text{C}=\text{C}$  radical and CH<sub>2</sub>O. (The  $\text{C}=\text{C}(\text{C})\text{CO}\cdot \rightarrow \text{C}=\text{C}(\text{C})\text{C}=\text{O} + \text{H}$  reaction path is also included in our mechanism.)

**Allylic Isobutenyl Radical ( $\text{C}=\text{C}(\text{C})\text{C}\cdot$ ) + O<sub>2</sub> Reaction System.** The potential energy diagrams for the chemical activation calculations of the O<sub>2</sub> +  $\text{C}=\text{C}(\text{C})\text{C}\cdot$  combination reactions are shown in Figure 2a and 2b. The  $\text{C}=\text{C}(\text{C})\text{C}\cdot$  undergoes addition with O<sub>2</sub> to form the chemically activated  $\text{C}=\text{C}(\text{C})\text{COO}\cdot$  adduct. The reaction channels of the  $\text{C}=\text{C}(\text{C})\text{COO}\cdot$  adduct include dissociation back to reactants, stabilization to  $\text{C}=\text{C}(\text{C})\text{COO}\cdot$  radical, isomerization via hydrogen shifts with subsequent  $\beta$ -scission or R•O–OH bond cleavage. The  $\text{C}=\text{C}(\text{C})\text{COO}\cdot$  adduct can also cyclize to four- or five-member cyclic peroxide-alkyl radicals. The reaction of  $\text{C}=\text{C}(\text{C})\text{COO}\cdot$  adduct to  $\text{C}=\text{C}(\text{C})\text{CO}\cdot + \text{O}$  atom is included for completeness, but it is only important at high temperature (above 1500 K). Figure 2a shows isomerizations via H shift and the  $\text{C}=\text{C}(\text{C})\text{CO}\cdot + \text{O}$  reaction paths; whereas isomerization pathways to form cyclic adducts are shown in Figure 2b.

**A. Comparison of Thermodynamic Properties Determined by Different Calculation Methods.** The important geometrical parameters, moments of inertia and values of spin containment for reactant, important intermediates and transition states calculated from MP2(full)/6-31g(d) and B3LYP/6-31g(d) are listed in Table 5. The optimized MP2(full)/6-31g(d) and B3LYP/6-31g(d) structures and frequencies for all species are available in the Supporting Information. Comparison with stable molecules between MP2(full)/6-31g(d) and B3LYP/6-31g(d) optimized geometries are in agreement. Differences of bond length are within 0.019 Å, bond angles are within 1.8°, and dihedral angles are within 9.7°. Vibrational frequencies are within  $\pm 5\%$  factor between MP2(full)/6-31g(d) and B3LYP/6-31g(d) calculations, with exception of two frequencies of C<sub>2</sub>•Y(CCOC) ( $\nu_6$ ) and C=Y(CCOC) ( $\nu_1$ ). Comparison MP2 and DFT geometries on TSs show larger differences for active site bond lengths.

MP2(full)/6-31g(d) and B3LYP/6-31g(d) determined frequencies are available in the Supporting Information. Torsion frequencies which correspond to internal rotors calculated from MP2(full)/6-31g(d) and B3LYP/6-31g(d) are not included in vibrational contributions for S<sub>298</sub> and Cp(T)'s. Torsion frequency contributions to S<sub>298</sub> and Cp(300) – Cp(1500) as determined from method of Pitzer and Gwinn's for internal

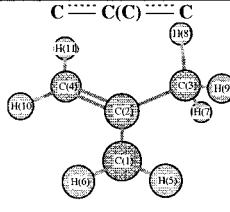
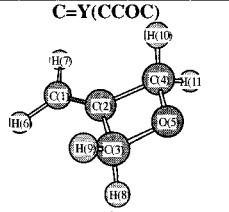
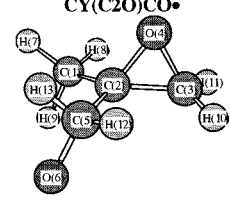
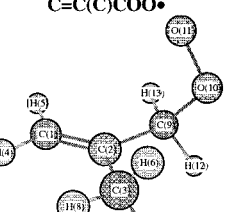
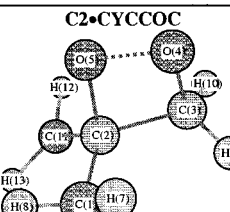
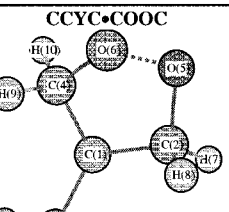
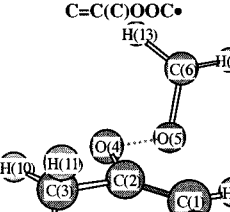
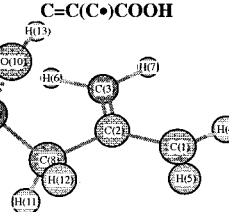
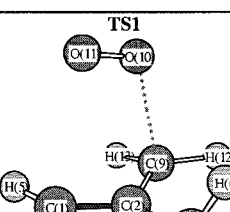
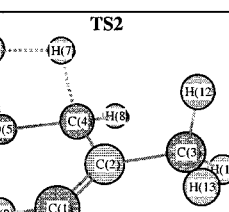


**Figure 2.** Potential energy diagrams for allylic isobutenyl radical ( $C=C(C)C\cdot + O_2$ ) combination reactions: (a) isomerizations via H shifts and  $C=C(C)CO\cdot + O$  atom paths; (b) cyclization pathways to form cyclic adducts and further reactions.

rotational contributions. Translational, rotational, and vibrational contributions are calculated from MP2(full)/6-31g(d) and B3LYP/6-31g(d) optimized geometries and frequencies. Comparison of the stable molecules indicates that MP2(full)/6-31g(d) and B3LYP/6-31g(d) determined  $S_{298}^\circ$  and  $Cp(T)$ 's are in agreement. Differences are within 1.06 cal/mol-K ( $S_{298}^\circ$  of CCYC•COOC) and 1.39 cal/mol-K ( $Cp(800\text{ K})$  of  $C=C(C)COOH$ ) for  $S_{298}^\circ$  and  $Cp(T)$ 's, respectively. Differences of MP2 and B3LYP-determined  $S_{298}^\circ$  and  $Cp(T)$ 's of TSs are within 3.23 cal/mol-K ( $S_{298}^\circ$  of TS4) and 2.19 cal/mol-K ( $Cp(500\text{ K})$  of TS2) for  $S_{298}^\circ$  and  $Cp(T)$ 's, respectively.

Comparison of the results of total energy (at 298 K) differences between TSs and reactants, intermediates, and products at various levels (Table 1) show that the density functional calculated values at the B3LYP/6-31g(d) and B3LYP/6-311+g(3df,2p)//B3LYP/6-31g(d) levels are lower than MP2(full)/6-31g(d) values. CBS calculations based on MP2(full)/6-31g(d) and B3LYP/6-31g(d) optimized geometries have similar results, where differences are within 4 kcal/mol except in the reaction of  $C=C(C)C\cdot + O_2 \rightarrow TS1 \rightarrow C=C(C)COO\cdot$ . Results of MP4(full)/6-31g(d,p)//MP2(full)/6-31g(d) calculations are between values of CBS-q//MP2(full)/

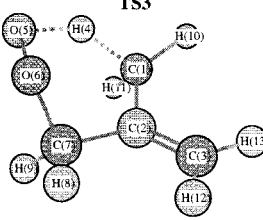
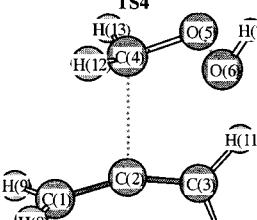
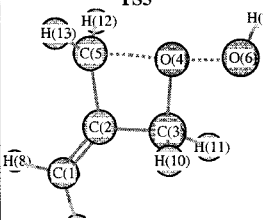
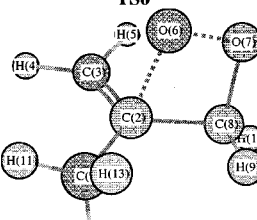
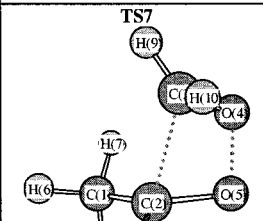
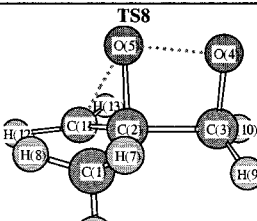
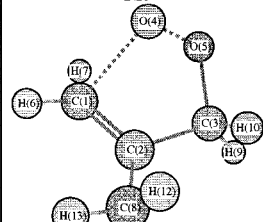
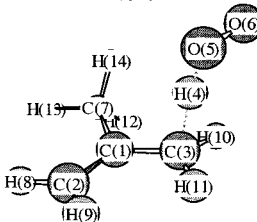
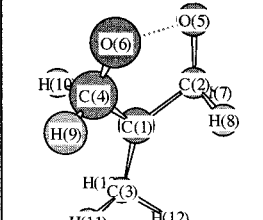
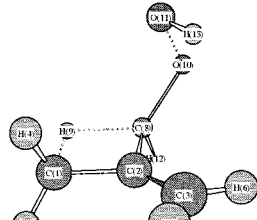
**TABLE 5: Structural Parameters for Transition States, Important Intermediates and Products of C<sup>≡</sup>C(C)≡C + O<sub>2</sub> Reaction System Calculated at MP2(full)/6-31g(d) and B3LYP/6-31g(d)**

Molecule	B3LYP	MP2	Molecule	B3LYP	MP2
 <p>182.1, 205.5, 376.3<sup>b</sup> 179.2, 203.5, 371.5</p>	r21 <sup>a</sup> r32 r42 a321 a421 d4213 S <sup>2</sup> S <sup>2</sup> A <i>S<sup>2</sup>A-qcisd(t)</i>	1.3901 1.5194 1.5117 1.3901 1.3794 119.29 121.17 178.56 0.961 0.758 0.759	 <p>151.4, 385.7, 514.0 151.2, 385.1, 513.2</p>	r21 r32 r42 r53 a321 a421 a532 d4213 d5321	1.3259 1.5141 1.5107 1.4501 136.49 136.25 90.54 180.00 180.00
 <p>314.1, 611.3, 749.0 313.1, 606.8, 739.5</p>	r21 r32 r43 r52 r65 a321 a432 a521 a652 d4321 d5213 d6521 S <sup>2</sup> S <sup>2</sup> A	1.5101 1.4719 1.4646 1.4366 1.5285 1.5115 1.3659 121.45 116.19 115.08 103.80 203.70 57.16 0.758 0.75	 <p>315.1, 726.5, 836.4 315.2, 704.7, 804.4</p>	r21 r32 r92 r109 r1110 a321 a921 a1092 a11109 d9213 d10921 d111092 S <sup>2</sup> S <sup>2</sup> A <i>S<sup>2</sup>A-qcisd(t)</i>	1.3360 1.5072 1.5037 1.4718 1.3224 123.59 120.06 111.72 111.14 179.35 121.27 288.85 0.765 0.75 0.751
 <p>327.5, 528.2, 591.7 326.4, 520.8, 584.8</p>	r21 r32 r43 r54 r112 a321 a432 a543 a1121 d4321 d5432 d11213 S <sup>2</sup> S <sup>2</sup> A <i>S<sup>2</sup>A-qcisd(t)</i>	1.5232 1.5409 1.4401 1.4925 1.4736 113.85 89.99 88.10 114.17 269.62 341.00 140.37 0.756 0.75 0.761	 <p>254.5, 575.9, 775.8 255.5, 568.9, 761.5</p>	r21 r31 r41 r52 r56 r64 a312 a412 a521 a641 d4123 d5213 d6412 S <sup>2</sup> S <sup>2</sup> A <i>S<sup>2</sup>A-qcisd(t)</i>	1.4966 1.4871 1.4993 1.4284 1.470 1.4312 126.33 105.25 104.29 104.65 163.96 179.83 348.87 0.754 0.75 0.75
 <p>234.5, 766.5, 923.3 240.8, 741.6, 885.0</p>	r21 r32 r42 r54 r65 a321 a421 a542 a654 d4213 d5421 d6542 S <sup>2</sup> S <sup>2</sup> A <i>S<sup>2</sup>A-qcisd(t)</i>	1.3322 1.5115 1.3831 1.4645 1.3611 126.56 126.07 110.97 107.97 180.22 2.17 243.53 0.754 0.75 0.75	 <p>299.2, 736.1, 805.7 302.6, 718.4, 779.1</p>	r21 r32 r82 r98 r109 r1310 a821 a982 a1098 a13109 d8213 d9821 d10982 d131098 S <sup>2</sup> S <sup>2</sup> A <i>S<sup>2</sup>A-qcisd(t)</i>	1.3867 1.3912 1.5254 1.4218 1.4523 0.9767 118.66 113.57 107.21 100.67 178.98 145.06 290.67 89.82 0.782 0.75 0.759
 <p>356.0, 757.6, 832.4 335.5, 695.2, 773.5</p>	r21 r32 r92 r109 r1110 a321 a921 a1092 a11109 d9213 d10921 d111092 S <sup>2</sup> S <sup>2</sup> A <i>S<sup>2</sup>A-qcisd(t)</i>	1.3755 1.5156 1.3986 2.3636 1.2350 121.01 117.45 99.83 112.27 192.53 71.43 328.07 1.613 1.152 1.148	 <p>250.6, 808.2, 946.0 251.1, 773.5, 908.0</p>	r21 r32 r42 r54 r65 r74 r76 a21 a542 a654 a742 d4213 d5421 d6542 d7421 S <sup>2</sup> S <sup>2</sup> A <i>S<sup>2</sup>A-qcisd(t)</i>	1.3488 1.5102 1.4651 1.3910 1.4929 1.294 1.329 120.63 118.26 90.35 113.48 181.41 351.16 119.36 89.81 0.772 0.75 0.791

<sup>a</sup> Geometry r: bond length in Å; a: bond angle in degree; d: dihedral angle in degree. <sup>b</sup> Moments of inertia in amu. Bohr<sup>2</sup>, italic: calculated at B3LYP/6-31g(d). <sup>c</sup> S<sup>2</sup>: spin contamination from B3LYP/6-31g(d) and MP2(full)/6-31g(d); S<sup>2</sup>A: after annihilation S<sup>2</sup>; *S<sup>2</sup>A-qcisd(t)* spin contamination after annihilation from single point calculation QCISD(T)/6-31g.



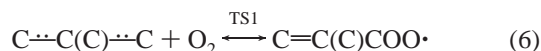
TABLE 5: (Continued)

 <p>292.1, 604.5, 786.9 281.0, 600.4, 793.9</p>	<p>r21 1.4516 1.4749 r32 1.3552 1.3120 r41 1.3899 1.3129 r54 1.2069 1.2145 r65 1.4041 1.4074 r72 1.514 1.507 r76 1.4426 1.4365 a412 95.76 98.28 a541 146.47 145.99 a654 101.16 101.45 a765 107.80 106.17 d4123 230.05 219.03 d5412 315.87 318.73 d6541 51.65 53.67 d7654 306.95 303.74 S<sup>2</sup> 0.773 1.051 S<sup>2</sup>A 0.750 0.804 S<sup>2</sup>A-qcisd(t) 0.772 0.772</p>	 <p>288.9, 889.4, 1015.8 303.1, 937.4, 1059.3</p>	<p>r21 1.3399 1.3227 r32 1.3152 1.2839 r42 2.3339 2.2327 r54 1.3649 1.3792 r65 1.4664 1.4741 r76 0.9749 0.9780 a321 157.15 159.82 a421 103.96 101.71 a542 113.81 113.48 a654 107.27 106.00 a765 98.32 97.69 d4213 178.27 179.03 d5421 166.14 172.80 d6542 285.15 282.44 d7654 215.08 223.97 S<sup>2</sup> 0.778 1.06 S<sup>2</sup>A 0.75 0.803 S<sup>2</sup>A-qcisd(t) 0.830 0.830</p>
 <p>204.5, 856.7, 1000.3 188.3, 815.5, 977.4</p>	<p>r21 1.3397 1.3022 r32 1.5000 1.4979 r43 1.4471 1.4556 r52 1.4625 1.4873 r54 1.969 1.851 r64 1.7384 1.5807 r76 0.9743 0.9734 a321 129.90 131.29 a432 93.99 95.53 a521 128.65 130.48 a643 101.14 100.21 a764 92.73 97.45 d4321 220.41 180.52 d5213 197.20 179.88 d6432 179.58 176.93 d7643 214.84 138.89 S<sup>2</sup> 0.809 0.978 S<sup>2</sup>A 0.751 0.779 S<sup>2</sup>A-qcisd(t) 0.798 0.798</p>	 <p>330.6, 562.3, 610.3 319.4, 554.9, 603.0</p>	<p>r21 1.5051 1.4962 r32 1.3939 1.3549 r62 1.8499 1.9002 r76 1.4484 1.4177 r82 1.534 1.524 r87 1.4284 1.4261 a321 120.83 121.13 a532 120.93 120.89 a621 106.51 107.92 a762 84.47 82.96 a876 95.13 94.93 d4321 18.29 12.62 d5321 189.16 185.37 d6213 114.70 110.48 d7621 131.77 136.49 d8762 343.25 337.76 S<sup>2</sup> 0.778 0.937 S<sup>2</sup>A 0.75 0.767 S<sup>2</sup>A-qcisd(t) 0.778 0.778</p>
 <p>335.2, 549.6, 618.0 331.2, 536.4, 607.5</p>	<p>R21 1.5183 1.5054 r32 1.9673 2.0153 r43 1.3744 1.3997 r52 1.4340 1.4386 r112 1.3753 1.3482 a321 104.57 103.18 a432 81.15 77.09 a521 113.78 113.91 a1121 121.76 123.67 d4321 271.14 274.58 d5213 277.97 282.12 d11213 134.19 133.02 S<sup>2</sup> 0.798 1.018 S<sup>2</sup>A 0.751 0.77 S<sup>2</sup>A-qcisd(t) 0.777 0.777</p>	 <p>338.4, 511.6, 597.0 336.5, 529.6, 592.0</p>	<p>r21 1.5189 1.5146 r32 1.5332 1.5176 r43 1.4291 1.4331 r52 1.4444 1.4528 r54 1.764 1.808 r112 1.4637 1.4791 r115 2.071 1.808 a432 93.79 93.78 a521 113.26 110.88 a1121 116.94 114.22 d4321 264.00 272.49 d5213 255.47 257.27 d11213 151.81 140.52 S<sup>2</sup> 0.876 1.541 S<sup>2</sup>A 0.751 0.751 S<sup>2</sup>A-qcisd(t) 0.791 0.791</p>
 <p>272.9, 595.2, 746.0 272.7, 579.6, 717.5</p>	<p>r21 1.3910 1.3576 r32 1.5173 1.5100 r41 1.9669 1.9625 r53 1.428 1.429 r54 1.4175 1.4089 r82 1.4948 1.4906 a321 112.06 112.61 a412 89.24 87.23 a541 90.79 89.90 a821 124.89 125.02 d4123 324.55 320.33 d5412 54.52 58.43 d8213 159.93 160.08 S<sup>2</sup> 0.789 0.826 S<sup>2</sup>A 0.75 0.751 S<sup>2</sup>A-qcisd(t) 0.775 0.775</p>	 <p>306.1, 1160.1, 1291.8 300.0, 1049.5, 1189.0</p>	<p>r21 1.3693 1.3363 r31 1.4278 1.4417 r43 1.5250 1.3820 r54 1.1130 1.1752 r65 1.2990 1.2818 r71 1.5140 1.5045 a431 105.59 104.63 a543 170.69 166.38 a654 107.01 106.35 d4312 258.47 253.74 d5431 238.64 258.77 d6541 256.65 272.92 d7123 182.19 182.68 S<sup>2</sup> 2.03 2.24 S<sup>2</sup>A 2.0 2.018 S<sup>2</sup>A-qcisd(t) 2.018 2.018</p>
 <p>318.5, 529.9, 754.0</p>	<p>r21 1.4940 1.4974 r31 1.4827 1.3045 r41 1.4893 1.5060 r52 1.3781 1.3934 r56 1.959 1.3919 r64 1.3630 1.3455 a312 125.20 94.63 a412 109.88 81.28 a521 99.10 80.51 a641 109.79 121.87 d4123 195.61 108.46 d5213 119.87 181.09 d6412 3.27 4.20 S<sup>2</sup> 0.85 0.842 S<sup>2</sup>A 0.751 0.755 S<sup>2</sup>A-qcisd(t) 0.761 0.761</p>	 <p>333.7, 701.4, 788.0 336.7, 668.5, 744.0</p>	<p>r21 1.4989 1.4974 r32 1.3345 1.3045 r82 1.5032 1.5060 r98 1.4089 1.3934 r108 1.3835 1.3919 a321 133.40 134.55 a821 96.05 94.63 a982 81.28 80.51 a1082 121.87 119.30 a11108 108.46 106.89 d8213 181.09 184.08 d9821 1.33 4.20 S<sup>2</sup> 0.762 0.842 S<sup>2</sup>A 0.75 0.755 S<sup>2</sup>A-qcisd(t) 0.761 0.761</p>

6-31g(d) and MP2(full)/6-31g(d) calculations. We choose the values of CBS-q//MP2(full)/6-31g(d) and B3LYP/6-311+g(3df,2p)//B3LYP/6-31g(d) calculations for further discussion; data in parentheses are from B3LYP/6-311+g(3df,2p)//B3LYP/6-31g(d) calculations.

Several transition states, specifically TS1 and TS4 show high spin contamination, which suggests possible error in the TS enthalpy, see  $\langle S^2 \rangle$  data in Table 4. The CBS-q method uses a QCISD(T)/6-31G calculation to provide a spin correction. The projected  $\langle S^2 \rangle$  values for the QCISD(T) calculations on the MP2 geometry's are below 0.8 for most TS's; with TS1 showing  $\langle S^2 \rangle$  of 1.15 and TS4 at 0.83. TS1 is important and we choose a barrier in agreement with the experimental data. TS4 shows a barrier of 2 to 5 kcal/mol for addition of an alkyl radical to ketene, this appears about 3–5 kcal/mol low, but the alkyl radical,  $C\cdot H_2OOH$ , is dissociating (with no barrier) to lower energy products  $CH_2O + OH$ . Maranzana et al.<sup>100</sup> have recently shown that density functional calculations yield similar results to multireference perturbation theory in reactions of  $O_2$  ( $^1\Delta_g$ ) with several unsaturates.

**B. Formation of Allylic Isobutenyl Peroxy Radical ( $C=C(C)COO\cdot$ ).**  $\Delta H_f^\circ$  ( $C\cdot C(C)C$ ) is calculated to be 32.56 (32.81) kcal/mol from  $\Delta H_f^\circ$  ( $C=C(C)C$ ) and bond enthalpy ( $C=CC-H$ ) using isodesmic reaction (IR1).  $\Delta H_f^\circ$  ( $C=C(C)COO\cdot$ ) is determined to be 11.06 (10.79) kcal/mol using  $\Delta H_f^\circ$  ( $C=C(C)COOH$ ) (–24.51 (–23.85) kcal/mol from isodesmic reaction IR2) and bond enthalpy ( $C=C(C)COO-H$ ) (87.66 (86.74) kcal/mol from isodesmic reaction IR3).



The barriers for this reaction 6 calculated from MP2 versus B3LYP transition state structures show significant deviation. We find a small barrier of 1.47 kcal/mol based on CBS-q//MP2(full)/6-31g(d), 12.22 kcal/mol based on CBS-q//B3LYP/6-31g(d) and no barrier based at B3LYP/6-311+g(3df,2p)//B3LYP/6-31g(d) for reaction 6 in the forward direction. The difference in the CBS-q values for these two geometries results from a 9 kcal/mol difference in the empirical correction between CBS-q//B3LYP/6-31g(d) and CBS-q//MP2(full)/6-31g(d) calculations.

$\Delta E(\text{empirical correction}) =$

$$-0.00594 \sum_i \left( \sum_{\mu=1}^{N_{ii}} C_{\mu ii} \right)^2 |S|_{ii}^2 - 0.00403(n_\alpha + n_\beta)$$

where  $(\sum C_{\mu ii})^2$  is the interference factor;  $|S|_{ii}$  is the absolute overlap integral;  $n_\alpha$  and  $n_\beta$  are the numbers of spin-up and spin-down valence electrons.<sup>13–15</sup>

There is a  $\sim 0.4$  Å difference between MP2(full)/6-31g(d) and B3LYP/6-31g(d) optimized geometries for the active site C–O bond length of TS1. There is also a factor  $\sim 7$  difference between MP2(full)/6-31g(d) and B3LYP/6-31g(d) calculated imaginary frequency at TS1, 862 and 119  $cm^{-1}$  respectively. The transition state obtained from B3LYP/6-31g(d) calculation has a loose geometry relative to the structure from MP2(full)/6-31g(d).

The Arrhenius pre-exponential factor,  $A_\infty$ , is calculated via canonical TST. The high-pressure limit rate constants, fit by a three parameters ( $A$ ,  $n$ ,  $E_a$ ) modified Arrhenius equation over a temperature range of 300 K to 2000 K, are  $1.09 \times 10^{10} T^{0.57} \exp(-2291 \text{ cal}/RT)$  ( $cm^3 \text{ mol}^{-1} \text{ s}^{-1}$ ) and  $4.65 \times 10^8 T^{1.19} \exp(-534 \text{ cal}/RT)$  ( $cm^3 \text{ mol}^{-1} \text{ s}^{-1}$ ) at CBS-q//MP2(full)/6-

31g(d) and B3LYP/6-311+g(3df,2p)//B3LYP/6-31g(d), respectively. The experimental rate constants reported by Jenkin et al.,<sup>34</sup>  $3.61 \times 10^{11}$  ( $cm^3 \text{ mol}^{-1} \text{ s}^{-1}$ ) (at 296 K), Slagle et al.,<sup>35</sup>  $<3.01 \times 10^{10}$  ( $cm^3 \text{ mol}^{-1} \text{ s}^{-1}$ ) (at 600 K), and Ruiz et al.,<sup>36</sup>  $9.51 \times 10^{10}$  ( $cm^3 \text{ mol}^{-1} \text{ s}^{-1}$ ) (at 348 K) indicate there is no significant barrier for the similar reaction of allyl radical +  $O_2 \rightarrow$  allylperoxy radical. These experimental evaluations do have low  $A$  factors suggesting that small barriers may exist; but they also clearly exclude any barrier of more than a few kcal/mol. The calculated barrier of 1.47 kcal/mol at CBS-q//MP2(full)/6-31g(d) level is plausible; but not the value of 12 kcal/mol calculated at CBS-q//B3LYP/6-31g(d) level. Higher level calculations for this reaction result in barriers are 0.56 and 3.4 kcal/mol at CBS-Q//MP2(full)/6-31g(d) and CBS-Q//B3LYP/6-31g(d) respectively with small negative value for the TS enthalpy relative to reactants at B3LYP/6-311+g(d,p)//B3LYP/6-31g(d) and G3MP2 levels.

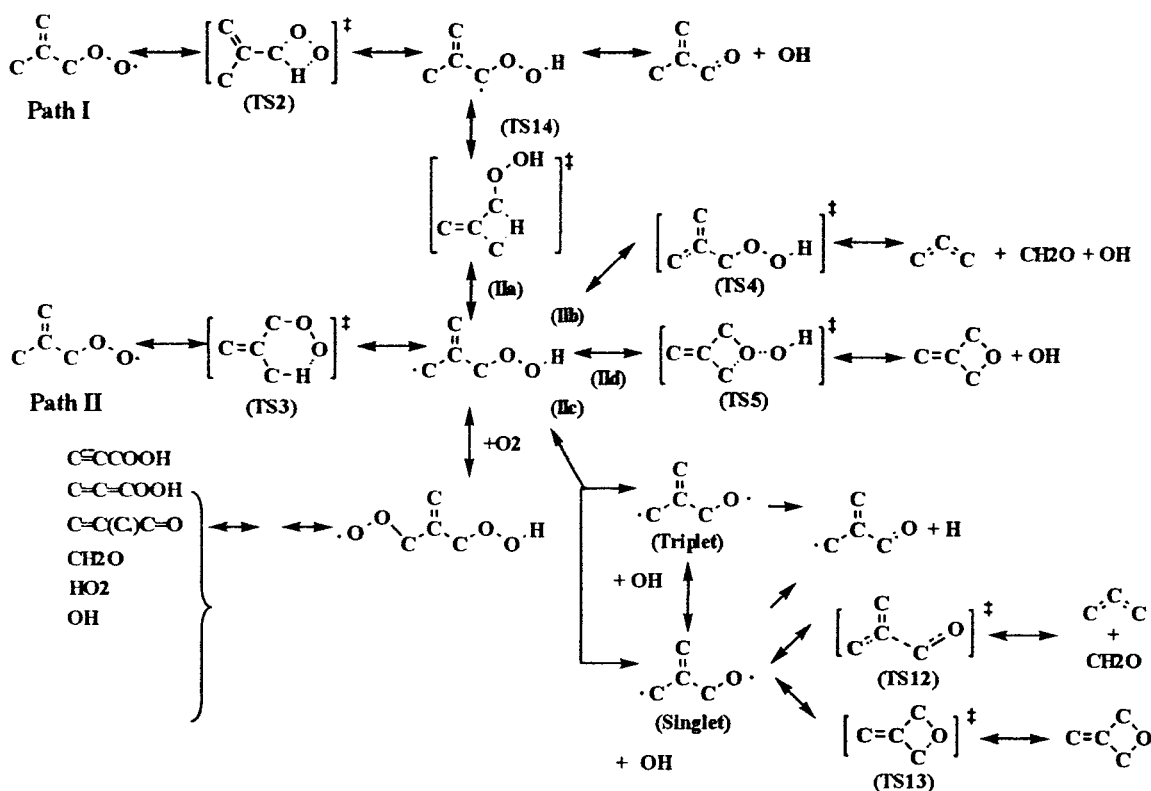
The well depth (ca. 21 kcal/mol) for  $C\cdot C(C)C + O_2 \rightleftharpoons C=C(C)COO\cdot$  is low relative to alkyl radical +  $O_2$  systems (ca. 35 kcal/mol). This is due to a loss of resonance stabilization and places the reaction barriers to new product channels 6.7 (3.0) kcal/mol or more higher than dissociation back to reactants. One exception is the formation of the  $C=C(C)COOH$  isomer via a six-member cyclic transition state structure, TS3, with barrier of only 19.82 (19.60) kcal/mol relative to the stabilized  $C=C(C)COO\cdot$  adduct. This isomer has significant barriers to further reactions, however. It requires 42.14 (32.00) kcal/mol (via TS5), 51.39 (53.01) kcal/mol (via TS4), 54.09 (51.64) kcal/mol (via TS14), and 42.45 (41.90) kcal/mol (in addition to the 19.82 (19.60) kcal/mol for isomerization) for further reaction to methylene oxirane + OH,  $C=C=C + C\cdot H_2OOH$ ,  $C=C(C)COOH$ , and  $C=C(C)CO\cdot + OH$ , respectively. These reactions will be further discussed, particularly the important channels to methylene oxirane + OH. The major reaction flux of  $C=C(C)COO\cdot$  is, therefore, back to the  $C=C(C)COO\cdot$  peroxy radical or further reaction with  $O_2$ .

We note that there are two electronic energy levels for the peroxy radical species ( $ROO\cdot$ ) which are ca. 23 kcal/mol different in energy.<sup>98</sup> High level calculations estimating these peroxy systems may select multireference calculation methods to include both of these electronic states. We note that we have had reasonable success in previous studies,<sup>38</sup> and the early single reference calculations (density functional) of Schaefer et al.<sup>99</sup> are well regarded. We feel that the composite Complete Basis Set (CBS-q) calculations on structures calculated with MP2 and density functional methods will further improve the energy estimation and provides a reasonable method for the many structures and reactions in this complex isobutenyl radical system.

The major reaction channel of the  $C=C(C)COO\cdot$  adduct is reaction back to  $C\cdot C(C)C + O_2$ . Other reactions for the stabilized  $C=C(C)COO\cdot$  adduct are isomerization (H-shift) pathways I, II and cyclization pathway IIIa and IIIb.

**C. Isomerization (H-Shift) Pathways I and II.** Scheme 1 shows that the first step of reaction paths I and II is intramolecular isomerization—hydrogen transfer—via TS2 and TS3 transition states, respectively. The H transfer step of reaction path I has a higher  $A$  factor of  $1.33 \times 10^{12}$  ( $2.14 \times 10^{12}$ )  $s^{-1}$  at 743 K but also a higher activation energy of 39.46 (37.62) kcal/mol than reaction path II (data below). This isomerization is the rate-determining step for reaction path I because the following  $\beta$ -scission forms a strong carbonyl bond, ( $C=O$ ), which has a low barrier to products, 1–2 kcal/mol and slightly higher  $A$  factor. Reaction path I occurs through a four-member

SCHEME 1



ring intramolecular H transfer and contributes to methacrolein product formation.

**Reactions of C=C(C)COOH Adduct.** The first step of reaction path II has a low activation energy 19.82 (19.60) kcal/mol, but the following reactions all involve high barriers. Reaction IIa (C=C(C)COOH → C=C(C)C·OOH) occurs isomerization via four-member ring (TS14) intramolecular hydrogen shift and requires 54.09 (51.64) kcal/mol with A factor of  $7.8 \times 10^{11}$  ( $1.62 \times 10^{12}$ ) s<sup>-1</sup>. This high barrier results from loss of resonance stabilization to form the TS (ca. 13 kcal/mol), strain for the four-member ring (ca. 28 kcal/mol) and a thermoneutral reaction barrier of ca. 13 kcal/mol (using an Evans Polanyi evaluation). Reaction IIb, β-scission to C=C=C + CH<sub>2</sub>O + OH, requires 51.39 (53.01) kcal/mol of which 47 kcal/mol is from the endothermicity. Reaction path IIc is an important new, chain branching reaction path. It involves cleavage of the weak peroxide bond, C=C(C)CO·····OH (bond fission), to form C=C(C)CO· biradical + OH. The C=C(C)COOH → C=C(C)CO· + OH channel has an A of  $4 \times 10^{15}$  s<sup>-1</sup> and requires 42.45 (41.90) kcal/mol to break R·O—OH bond. The A factor is estimated from reactions of ROOH → RO· + OH.<sup>37</sup> The barrier of 42.45 (41.90) kcal/mol is obtained from a best fit of our model to the experimental data; this value is close to experimental values of 41.4 ~ 42.92 kcal/mol for the reactions of ROOH → RO· + OH.<sup>50–55</sup>

We consider this C=C(C)COOH adduct dissociation to both triplet and singlet C=C(C)CO· biradicals. The calculated barriers are 41.64 and 40.61 kcal/mol for C=C(C)CO· (singlet) + OH and C=C(C)CO· (triplet) + OH channels, respectively, using B3LYP/6-31g(d) level. The calculated difference in singlet versus triplet enthalpies is 1.03 kcal/mol at B3LYP/6-31g(d) level; triplet is lower. The A factors for dissociation to triplet vs singlet would have ratio of 3:1. The singlet form is needed for reaction to methylene oxirane. Triplet to singlet conversion is included via collision with bath gas with a rate constant of  $5 \times 10^{13}$  s<sup>-1</sup>, ca. one-tenth collision rate. Using the mechanism

in CHEMKIN, we observe almost no difference in product formation (overall conversion <2%) between use of only one channel for the reaction, all reaction going to the singlet with  $E_a$  of 42.45 (41.90) kcal/mol ( $A = 4 \times 10^{15}$  s<sup>-1</sup>) versus use of reactions to both singlet and triplet with  $E_a$  of 42.22 (41.72) kcal/mol ( $A = 3 \times 10^{15}$  s<sup>-1</sup>) for triplet channel ( $E_a = 43.25$  (42.75) kcal/mol and  $A = 1 \times 10^{15}$  s<sup>-1</sup> for the singlet channel). For modeling purposes a single channel can represent the C=C(C)COOH ↔ C=C(C)CO· + OH reaction.

It is also important to evaluate other dissociation reaction paths of singlet C=C(C)CO· because this biradical can dissociate to two stable molecules (allene + CH<sub>2</sub>O) or undergo intramolecular ring closure to methylene oxirane. Three reaction paths are considered and included in the mechanism for this singlet C=C(C)CO· biradical:

(i) Intramolecular ring closure (via TS13) to form a four-member ring, methylene oxirane, product ( $\Delta H = -40$  kcal/mol). The reaction barrier of this singlet C=C(C)CO· → TS13 is calculated to be 1.72 kcal/mol at the CBS-q//B3LYP/6-31g(d) level with A factor of  $4.53 \times 10^{11}$  s<sup>-1</sup> at 800 K.

(ii) Dissociation (via TS12) to C=C=C + CH<sub>2</sub>O ( $\Delta H = -25.02$  kcal/mol). The barrier for singlet C=C(C)CO· → TS12 is determined as 6.41 kcal/mol at the CBS-q//B3LYP/6-31g(d) level with A factor of  $2.93 \times 10^{12}$  s<sup>-1</sup> at 800 K. This barrier results from rearrangement, (twist of methylene group), which involves loss of the allylic resonance.

(iii) H atom elimination to C=C(C)C=O radical form a carbonyl bond (C=O) ( $\Delta H = 11.62$  kcal/mol,  $E_a = 17.35$  kcal/mol).

Triplet C=C(C)CO· biradical β-scission to C=C(C)C=O radical + H atom reaction path is also included.

An alternate and more conventional pathway to methylene oxirane is intramolecular cyclization (reaction path IIc) via TS5 to form this oxirane + OH, which occurs via the alkyl carbon radical attack on the near peroxide oxygen atom (unimolecular)

with concerted cleavage of the weak O–OH peroxide bond. This reaction via TS5 has an  $A$  of  $6.95 \times 10^{11}$  ( $1.03 \times 10^{12}$ )  $s^{-1}$  (at 743 K) and an  $E_a$  of 42.14 (32.00) kcal/mol. Comparison of geometries for TS5 calculated from MP2(full)/6-31g(d) and B3LYP/6-31g(d), show the MP2-determined TS5 is near planar in structure, whereas B3LYP-determined TS5 is a chair structure (dihedral angle  $d5234 = 0.6^\circ$  in MP2 geometry and  $d5234 = 27^\circ$  in B3LYP geometry) (see Table 5). B3LYP-determined TS5 has longer bond lengths than MP2 at the active site bonds (bond length O4–C5 = 1.969 Å in B3LYP geometry (1.851 Å in MP2 geometry) and O6–O4 = 1.7384 Å in B3LYP geometry (1.5807 Å in MP2 geometry)). The CBS-q calculated barriers based on MP2 and B3LYP geometries result in similar enthalpies, even though the geometries are different on these two levels. The calculated barrier is ca. 42 kcal/mol based on CBS-q//MP2(full)/6-31g(d) and CBS-q//B3LYP/6-31g(d) calculations. The B3LYP/6-311+g(3df,2p)//B3LYP/6-31g(d) calculated barrier is ca. 10 kcal/mol lower than the CBS-q value and is not in agreement with loss of resonance in the TS and the thermochemical considerations discussed below.

We further evaluate this barrier, TS5, using thermochemical kinetics and comparison with other oxirane ring formation barriers. Calculation on the *n*-propyl radical + O<sub>2</sub> system<sup>90</sup> to formation of oxirane (four-member ring ether) + OH from the 3-hydroperoxide propyl radical (C•CCOOH) shows a barrier of 21.30 (18.30) kcal/mol and exothermicity of 10.43 (14.55) kcal/mol based on CBS-Q//B3LYP/6-31g(d,p) calculation. Data in parentheses are calculation at B3LYP/6-311+g(3df,2p)//B3LYP/6-31g(d,p). A comparable barrier using an Evans Polanyi evaluation where 1 kcal/mol reaction in barrier occurs for each 3 kcal/mol of exothermicity, for a thermoneutral reaction would be  $21.3 + 3.5 = 24.8$  kcal/mol and  $18.3 + 4.9 = 23.2$  kcal/mol based on CBS-Q//B3LYP/6-31g(d,p) and B3LYP/6-311+g(3df,2p)//B3LYP/6-31g(d), respectively. A second calculation on oxirane (a four-member ring) formation from methyl *tert*-butyl hydroperoxy ether radical<sup>39</sup> (C<sub>2</sub>•C(COOH)OC → C<sub>2</sub>Y(COCO)OC + OH) yields a barrier of 25.6 (19.50) kcal/mol at exothermicity of 12.53 (12.59) kcal/mol based on CBS-q//B3LYP/6-31g(d) calculation. Here, the barrier for thermoneutral reaction is estimated to be  $25.6 + 4.2 = 29.8$  kcal/mol and  $19.5 + 4.2 = 23.7$  kcal/mol, respectively.

The near thermoneutral reaction to form methylene oxirane ( $\Delta H_{rxn} = -0.67$  kcal/mol) from the allylic isobutenyl hydroperoxy radical, should have a 24 to 30 kcal/mol barrier (from thermochemical kinetic and Evans Polanyi analysis). An additional ca. 13 kcal/mol increase in the barrier is required for loss of resonance stabilization to form the TS. This thermochemical kinetic analysis yields:

- (i)  $24 + 13 = 37$  or
- (ii)  $30 + 13 = 43$  kcal/mol for the  $E_a$  of TS5.

The thermochemical analysis supports and we recommend the 42 kcal/mol; CBS-q calculated barrier.

CHEMKIN analysis with the reaction mechanism shows that the two chemical activation reaction paths IIc (intramolecular ring formation/OH elimination) and IIc (biradical + OH) are primarily responsible for methylene oxirane formation. Sensitivity analysis using the mechanism shows that path IIc (C=C(C•)COOH ↔ C=C(C•)CO• + OH ↔ C=Y(CCOC) + OH) contributes 99.97% and 64.9% of methylene oxirane at 743 K and 60 Torr, based on properties calculated from CBS-q//MP2(full)/6-31g(d) and B3LYP/6-31g(3df,2p)//B3LYP/6-31g(d), respectively.

Methylene oxirane formation has high sensitivity to the barrier of reaction path IIc, C=C(C•)COOH → C=C(C•)CO• + OH.

**TABLE 6: The Values of  $\Gamma$ s at 300, 743 and 1000 K**

$T$ (K)	TS2	TS3	TS14
300	3.0	4.2	6.9
743	1.2	1.2	1.3
1000	1.1	1.1	1.1

A decrease in this barrier by 0.5 kcal/mol (B3LYP/6-31g(3df,2p)//B3LYP/6-31g(d)) results in a ~16% of increase in the CHEMKIN analysis of methylene oxirane with a corresponding decrease of only ~2% in path IIc, reaction through TS5.

CHEMKIN analysis shows that the methylene oxirane formation is not significantly changed ( $< \pm 0.005\%$ ), when the  $E_a$  (CBS-q//MP2 values) for the high-pressure rate constant chemical activation reaction C=C(C•)COOH → TS5 → C=Y(CCOC) + OH is adjusted by  $\pm 1$  kcal/mol. The reaction of C=C(C•)COOH ↔ C=C(C•)CO• + OH is much faster than C=C(C•)COOH ↔ TS5 ↔ C=Y(CCOC) + OH. These chemical activation paths are important in combustion systems.

An asymmetric Eckart calculation of H tunneling as described in Schwartz et al.<sup>86,96–97</sup> is used to calculate the tunneling factor ( $\Gamma$ ) for H-shift isomerization (reactions through TS2, TS3 and TS14). The imaginary frequencies of TS2 (1027  $cm^{-1}$ ), TS3 (1082  $cm^{-1}$ ) and TS14 (1170  $cm^{-1}$ ), used in Eckart tunneling calculation are adjusted (down) from the MP2(full)/6-31g(d) determined imaginary frequency of 2334, 2460 and 2137  $cm^{-1}$  as recommended by Schwartz et al. The tunneling factors ( $\Gamma$ s) are in the range 6.9–1.0 from 300 to 2000 K. The values of  $\Gamma$ s at 300, 743 and 1000 K are given in Table 6. This tunneling influence on isomerization through TS2 and TS14 is ca. 1.0 kcal/mol in barrier at 300 K and 0.3 kcal/mol at 743 K, respectively. The effect is not significant compared to the two reaction barriers 40–50 kcal/mol (four-member H-shift reaction). The tunneling effect is more significant in isomerization through TS3 (six-member ring transition state) since this reaction barrier is much lower. But we note only small changes (less than  $6 \times 10^{-6}$  in mole fraction on acetone, methacrolein and 2,5-dimethylhexa-1, 5-diene product formations) that occur in the chemical activation analysis when the barriers are changed by 1 kcal/mol at 743 K.

**D. Cyclization (Formation of Four and Five-Member Ring) Pathway III.** Scheme 2 shows that reaction path III occurs via intramolecular addition of the terminal oxygen radical site to the C=C  $\pi$  bond, forming four- (reaction path IIIa) and five- (reaction path IIIb) member cyclic peroxide adducts. Reaction paths IIIa and IIIb are important to acetone formation. We note that the barriers for formation of the four- and five-member peroxides rings are higher by ca. 16 and 2 kcal/mol than reported earlier by Bozzelli and Dean<sup>31</sup> for the very similar allyl system. Activated energies for these two cyclizations are calculated as 28.20 (24.95) and 29.72 (27.98) kcal/mol with  $A$  factors of  $2.42 \times 10^{10}$  ( $3.28 \times 10^{10}$ ) and  $3.88 \times 10^{10}$  ( $6.09 \times 10^{10}$ )  $s^{-1}$  at 743 K, respectively, for five- and four-member ring cyclization. These high barriers 26–30 kcal/mol are required because the near complete loss of  $\pi$  bond energy for the terminal C double bond's twist that is needed to form the transition states. The low  $A$  factors result from the loss of 2 rotors in transition states.

The reaction OH addition to isobutene, then reaction of the hydroxyl adducts with O<sub>2</sub> is also important in acetone formation. This OH + isobutene → adduct + (O<sub>2</sub>) → products reaction system has been discussed in previous study.<sup>38</sup>

**QRRK Analysis on Chemical Activation Reaction System (C•C(C)•C + O<sub>2</sub>).** Input parameters and references to specific high-pressure rate constants for the chemical activation calculations on the reaction of C•C(C)•C + O<sub>2</sub> are listed in

## SCHEME 2

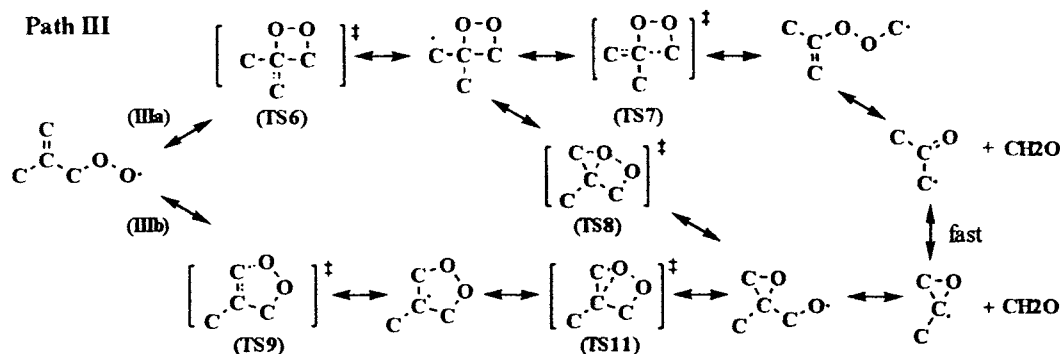


TABLE 7: Input Parameters and High-Pressure Limit Rate Constants ( $k_{\infty}$ ) for QRRK Calculation  $C=C(C)C\cdot + O_2 \rightarrow$  Products<sup>f</sup>

reaction	A (s <sup>-1</sup> or cm <sup>3</sup> /mol-s)	n	E <sub>a</sub> (kcal/mol)	ref
$C=C(C)C\cdot + O_2 \rightarrow C^*C(C)CQ\cdot$	$1.09 \times 10^{10}$ ( $4.65 \times 10^8$ )	0.56725 (1.18497)	2.29 (0.53)	a
$C^*C(C)CQ\cdot \rightarrow C=C(C)C\cdot + O_2$	$6.07 \times 10^{11}$ ( $1.42 \times 10^{12}$ )	0.60864 (0.60714)	23.29 (22.45)	a
$C^*C(C)CQ\cdot \rightarrow C^*C(C)CO\cdot + O$	$1.82 \times 10^{14}$	0.0	60.62	b
$C^*C(C)CQ\cdot \rightarrow C^*C(C)CO\cdot + OH$	$1.52 \times 10^9$ ( $3.96 \times 10^8$ )	1.02524 (1.30047)	39.46 (37.62)	a
$C^*C(C)CQ\cdot \rightarrow C^*C(C)CQ\cdot$	$1.41 \times 10^5$ ( $1.94 \times 10^5$ )	1.83586 (1.76544)	19.82 (19.60)	a
$C^*C(C)CQ\cdot \rightarrow C^*C(C)CQ\cdot$	$1.1 \times 10^{10}$ ( $8.23 \times 10^8$ )	0.14695 (0.50702)	20.76 (18.75)	a
$C^*C(C)CQ\cdot \rightarrow C^*CYCCOC + OH$	$6.82 \times 10^{12}$ ( $2.29 \times 10^{11}$ )	-0.34545 (0.22790)	42.14 (32.00)	a
$C^*C(C)CQ\cdot \rightarrow C^*C(C)CO\cdot + OH$	$4.0 \times 10^{15}$		42.45 (41.90)	
$C^*C(C)CQ\cdot \rightarrow C^*C^*C + C\cdot H_2OOH$	$1.18 \times 10^{12}$ ( $8.06 \times 10^{11}$ )	0.91203 (0.66482)	51.39 (53.01)	a
$C^*C(C)CQ\cdot \rightarrow C^*C(C)CO\cdot + OH$	$2.42 \times 10^9$ ( $3.97 \times 10^7$ )	0.87390 (1.60598)	54.09 (51.64)	a
$C^*C(C)CQ\cdot \rightarrow CCYC\cdot COOC$	$1.19 \times 10^8$ ( $2.56 \times 10^8$ )	0.80412 (0.73424)	28.02 (24.95)	a
$CCYC\cdot COOC \rightarrow C^*C(C)CQ\cdot$	$3.15 \times 10^{13}$ ( $4.88 \times 10^{12}$ )	-0.1293 (0.13537)	27.32 (24.33)	a
$CCYC\cdot COOC \rightarrow CCYCC\cdot OOC$	$3.56 \times 10^{13}$	0.0	38.82	c
$CCYCC\cdot OOC \rightarrow CCYC\cdot COOC$	$8.10 \times 10^{13}$	0.0	44.18	d
$CCYCC\cdot OOC \rightarrow CC(CO)\cdot CO$	$3.19 \times 10^{14}$	0.0	3.0	d
$CC(CO)\cdot CO \rightarrow CCYCC\cdot OOC$	$4.66 \times 10^{11}$	0.0	55.56	e
$CC(CO)\cdot CO \rightarrow CC\cdot C^*O + CH_2O$	$4.30 \times 10^{12}$	0.0	9.78	f
$CCYC\cdot COOC \rightarrow CCY(C_2O)\cdot CO\cdot$	$4.56 \times 10^{11}$ ( $4.56 \times 10^{11}$ )	0.92729 (0.64261)	17.47 (16.81)	g
$CCY(C_2O)\cdot CO\cdot \rightarrow CCYC\cdot COOC$	$6.92 \times 10^{11}$	0.061586	44.77 (47.04)	d
$CCY(C_2O)\cdot CO\cdot \rightarrow CCYC\cdot CO + CH_2O$	$1.74 \times 10^{13}$	0.0	18.15	f
$C^*C(C)CQ\cdot \rightarrow C_2\cdot CYCCOO$	$1.07 \times 10^8$ ( $1.30 \times 10^8$ )	0.89161 (0.93014)	29.72 (27.99)	a
$C_2\cdot CYCCOO \rightarrow C^*C(C)CQ\cdot$	$3.36 \times 10^{14}$ ( $7.41 \times 10^{12}$ )	-0.53625 (0.12151)	12.09 (8.72)	a
$C_2\cdot CYCCOO \rightarrow C^*C(C)COOC\cdot$	$4.41 \times 10^{13}$ ( $5.97 \times 10^{11}$ )	-0.22618 (0.56163)	18.50 (17.17)	a
$C^*C(C)COOC\cdot \rightarrow C_2\cdot CYCCOO$	$1.58 \times 10^{11}$ ( $2.14 \times 10^9$ )	-0.58296 (0.20485)	21.83 (18.69)	a
$C^*C(C)COOC\cdot \rightarrow C_2\cdot C^*O + CH_2O$	$1.41 \times 10^{10}$	0.0	1.0	h
$C_2\cdot CYCCOO \rightarrow CCY(C_2O)\cdot CO\cdot$	$1.21 \times 10^{13}$ ( $2.59 \times 10^{12}$ )	0.10180 (0.20895)	20.32 (12.52)	a
$CCY(C_2O)\cdot CO\cdot \rightarrow C_2\cdot CYCCOO$	$6.18 \times 10^{12}$ ( $1.32 \times 10^{12}$ )	-0.26947 (-0.16232)	64.55 (59.97)	a

<sup>a</sup> Fit with three parameter modified Arrhenius equation; A, estimated using canonical TST and MP2-determined entropies, E<sub>a</sub> evaluated from CBS-q/MP2(full)/6-31G(d) calculation. (Data in parentheses are from B3LYP-determined entropies and B3LYP/6-311+g(3df/2p)/B3LYP/6-31g(d) calculation.) <sup>b</sup> Estimated from O + CH<sub>3</sub>O. <sup>c</sup> A, estimated using TST, four equivalent H's, E<sub>a</sub> evaluated from ring strain (28.0) + E<sub>a</sub> abstraction (10.8). <sup>d</sup> ⟨MR⟩. <sup>e</sup> A, estimated using TST, loss of two rotors, symmetry; one equivalent H's, E<sub>a</sub> evaluated from ring strain (3.0) + ΔH<sub>rxn</sub> (52.56). <sup>f</sup> Estimated from C<sub>2</sub>H<sub>4</sub> + CH<sub>3</sub>. <sup>g</sup> A, estimated using canonical TST and B3LYP-determined entropies. E<sub>a</sub> evaluated from CBS-q/B3LYP/6-31G(d) calculation. (Data in parentheses are from B3LYP-determined entropies and B3LYP/6-311+g(3df/2p)/B3LYP/6-31g(d) calculations.) <sup>h</sup> Estimated from CO + CH<sub>3</sub>O. Geometric mean frequency (from CPFIT ref 26). C<sup>\*</sup>C(C)CQ<sup>\*</sup>: 359.6 cm<sup>-1</sup> (9.831), 1312.5 cm<sup>-1</sup> (13.523), 3164.2 cm<sup>-1</sup> (8.146). C<sup>\*</sup>C(C)CQ: 250.1 cm<sup>-1</sup> (7.359), 1046.9 cm<sup>-1</sup> (16.965), 2873.1 cm<sup>-1</sup> (6.677). CCYC·COOC: 447.7 cm<sup>-1</sup> (9.694), 1289 cm<sup>-1</sup> (15.604), 3077.4 cm<sup>-1</sup> (7.201). C<sub>2</sub>·CYCCOO: 437.4 cm<sup>-1</sup> (10.563), 1233.5 cm<sup>-1</sup> (14.718), 3142.2 cm<sup>-1</sup> (6.718). Lennard-Jones parameters: σ = 5.5471 Å, ε/k = 584.86 K (ref 28).

Table 7. The parameters in Table 7 are referenced to the ground (stabilized) level of the complex, as this is the formalism used in QRRK theory. Figure 3a and 3b illustrates the predicted effect of temperature and pressure on  $C=C(C)C\cdot + O_2$  reactions based on CBS-q/MP2(full)/6-31g(d) calculations. The data show that at low pressure and high-temperature most of the energized complex reacts back to reactants ( $C=C(C)C\cdot + O_2$ ); stabilization to  $C=C(C)COO\cdot$  and  $C=C(C)COOH$  adducts are dominant at low temperature and high pressure. Figure 3a indicates  $C=C(C)COO\cdot$  primarily undergoes reverse dissociation and O–O bond fission to a biradical  $C=C(C)CO\cdot + OH$  above 1200 K. Below 600 K, the major reaction is stabilization to  $C=C(C)COO\cdot$  and reverse reaction (back to reactants), which

dominates stabilization to  $C=C(C)COOH$  by ca. 2 orders of magnitude. The biradical  $C=C(C)CO\cdot + OH$  formation channel competes with the  $CY(C\cdot CO) + CH_2O$  channel ( $C=C(C)COO\cdot$  reaction through TS9, then through TS11), where  $CY(C\cdot CO)$  can further react to acetone radical ( $C=C(C)C\cdot O$ ) + CH<sub>2</sub>O. The concentration of  $C=C(C)COO\cdot$  is controlled by equilibrium, not by formation rate from reactants. Rate constants for product formation channels increase with increasing temperature and decreasing pressure. The product formations are controlled by the slower reactions out of the equilibrium systems. The near steady-state levels of  $C=C(C)COO\cdot$  and  $C=C(C)COOH$  make the reaction paths of  $C=C(C)COOH$  with O<sub>2</sub> important and they need to be included in the reaction mechanisms.

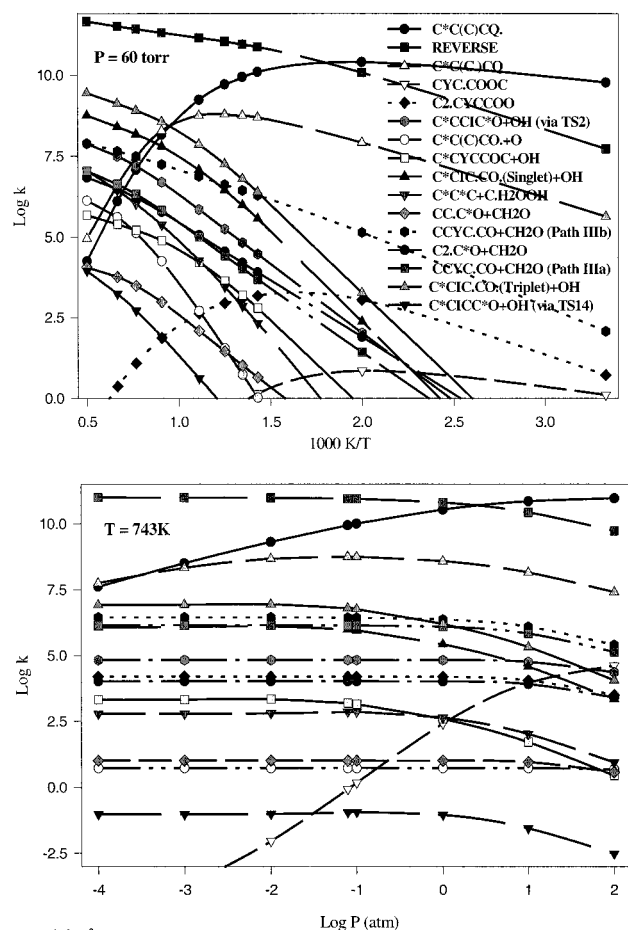


**Figure 3.** Calculated rate constants at different temperature and pressures for chemically activated reactions: allylic isobutenyl radical ( $C^{\cdot\cdot}C(C)C^{\cdot\cdot} + O_2 \Rightarrow [C=C(C)COO^*] \Rightarrow$  products). (a) Pressure at 60 Torr. (b) Temperature at 743 K.

All the reaction pathways of allylic isobutenyl radical with  $O_2$  involve barriers, that are above the energy of the initial reactants, because of the shallow well (21.5 kcal/mol) resulting from loss of the resonance stabilized radical. Alkyl radical reactions have well depths of 32–37 kcal/mol and the activated complex initially formed has more energy for further reaction to products (chemical activation paths). This explains why the  $C^{\cdot\cdot}C(C)C^{\cdot\cdot}$  shows very low reactivity toward  $O_2$ , and partially explains the high antiknock behavior in internal combustion engines of isobutene. Alkyl radicals reactions with isobutene form alkanes plus the allylic isobutenyl radical; this serves to cap the active alkyl radical and form a nonreactive isobutenyl radical.

Analysis of error resulting from inaccurate barrier to formation of the peroxy adduct and on the QRRK chemical activation results is performed by varying several barriers and observing changes in both the QRRK and the CHEMKIN results. A decrease of 1.0 in the 1.5 kcal/mol barrier for  $C^{\cdot\cdot}C(C)C^{\cdot\cdot} + O_2 \leftrightarrow C=C(C)COO^*$ , results in a calculated rate constant increase of 1.3, for forward reaction and a 1.7 increase for reverse at 743 K. Other product formations rate constants show no significant change. CHEMKIN analysis shows a very small decrease (less than  $1 \times 10^{-6}$  mol fraction) in acetone, methacrolein and 2,5-dimethylhexa-1,5-diene formation.

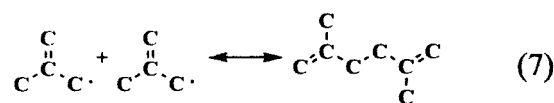
A decrease in the  $E_a$  of 1 kcal/mol for the important reaction of five member ring cyclization  $C=C(C)COO^* \leftrightarrow CCYC\cdot COOC$ , only effects the product formation channels resulting from the  $CCYC\cdot COOC$  intermediate. CHEMKIN analysis shows the lower barrier increases acetone formation by 4.6  $\times$

$10^{-5}$ , whereas other products decrease by ca.  $1.0 \times 10^{-5}$  in mole fraction, no observable change predicted.

The rate constants in the form of  $k = AT^n \exp(-E_a/RT)$  for the QRRK calculated chemical activation and unimolecular dissociation reactions at pressures of 0.076, 0.76, 7.6, 60, 760, and 7600 Torr over the temperature range 300 to 2000 K are available in the Supporting Information.

**Other Important Reactions of Allylic Isobutenyl Radical ( $C^{\cdot\cdot}C(C)C^{\cdot\cdot}$ ).** Concentrations of allylic isobutenyl radical can build up in reaction systems because it is resonantly stabilized and has low reactivity to new product formation via reaction with  $O_2$ , where dissociation of the peroxy radical back to  $C^{\cdot\cdot}C(C)C^{\cdot\cdot} + O_2$  is dominant. The concentration of allylic isobutenyl radical accumulates to relatively high levels and the radical is consumed mainly through radical–radical processes. The reaction mechanism and the CHEMKIN code are used to perform sensitivity analysis on reactions that control the formation of important products: acetone, methacrolein, methylene oxirane and 2,5-dimethylhexa-1,5-diene in isobutene oxidation.

**A.  $C^{\cdot\cdot}C(C)C^{\cdot\cdot} + C^{\cdot\cdot}C(C)C^{\cdot\cdot}$  Combination (Formation of 2,5-Dimethylhexa-1,5-diene).** 2,5-Dimethylhexa-1,5-diene is one of major products in this moderate temperature isobutene oxidation; it is formed via combination reaction 7. The behavior is in stark contrast to that of ethyl radicals and, in general, most alkyl radicals. For example, in the oxidation of propanal, which is an excellent source of ethyl radicals, oxidation at 673–793 K yields only minute traces of butane.<sup>40</sup> We use  $1.2 \times 10^{13}$  ( $cm^3 mol^{-1} s^{-1}$ )<sup>33</sup> for the high-pressure limit rate constant of reaction 7.



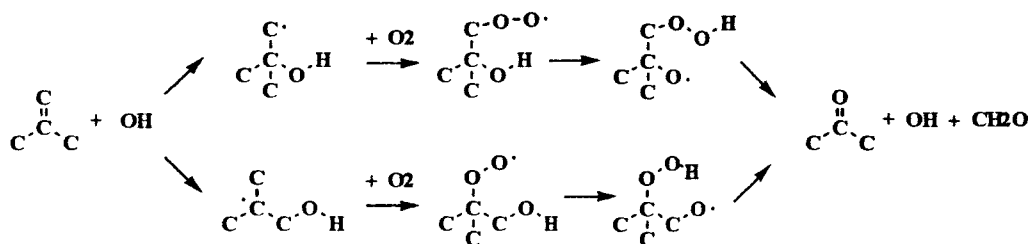
**B. Reaction with  $HO_2$ .** The  $HO_2$  radical is also relatively nonreactive and is an important intermediate in low to moderate temperature (below 1200 K) combustion. There are three exothermic paths of  $HO_2$  reactions with hydrocarbon radicals:

- (i) Hydroperoxide adduct formation
- (ii) Alkoxy radical + OH (dissociation of the weak RO–OH bond)
- (iii) Abstraction to form RH +  $O_2$ . This abstraction reaction is treated above as reverse of  $O_2 + RH$  in this isobutene study.

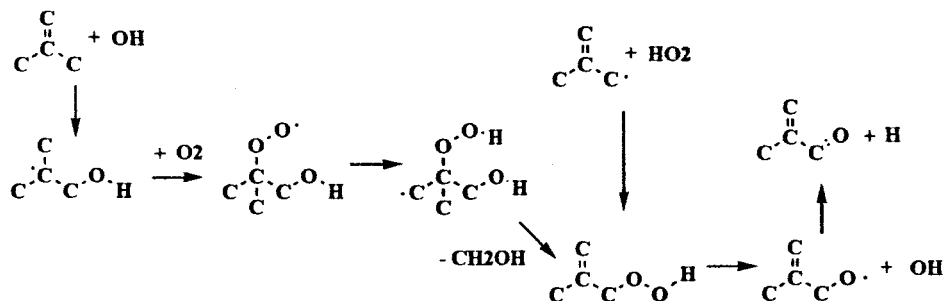
The association reaction of  $C^{\cdot\cdot}C(C)C^{\cdot\cdot}$  with  $HO_2$  forms an energized hydroperoxide adduct which cleaves the very weak RO–OH peroxide bond before stabilization occurs and forms an alkoxy radical. The alkoxy radical here can undergo one of two  $\beta$ -scission reactions: H atom elimination to produce methacrolein or formation of  $C-C=O$  radical and  $CH_2O$ .

**Reactions of Isobutene Important to Acetone Formation.** Acetone is the major product in oxidation of isobutene, with two important reaction pathways responsible for its formation. One is through OH radical addition to isobutene, then addition of  $O_2$  to this hydroxyl adduct. This overall reaction sequence is often referred to as the Waddington mechanism; two carbonyls are formed plus OH regeneration from reaction of OH with an olefin (shown in Scheme 3). The important reaction path of the peroxy-hydroxyl adduct is H transfer, from the hydroxyl to the peroxy group, aided by hydrogen bond ( $ROO\cdots H\cdots OR'$ ) formation. The H bond reduces the barrier for H shift isomerization by up to 4 kcal/mol.<sup>95</sup> The intermediate oxy radical rapidly decomposes to acetone plus formaldehyde and regenerates the reactive OH radical. Sensitivity analysis shows that a

SCHEME 3



SCHEME 4



decrease in barrier of this H shift isomerization (with H-bond stabilization) by 2 kcal/mol, results in increase of acetone formation by 30%. Methacrolein, 2,5-dimethylhexa-1,5-diene, and methylene oxirane formations change slightly (<2%).

The second important reaction pathway for acetone formation is from the reactions of allylic isobutenyl radical with O<sub>2</sub> (reaction pathway III of the C=C(C)C + O<sub>2</sub> reaction system).

OH radical formation from H<sub>2</sub>O<sub>2</sub> dissociation (H<sub>2</sub>O<sub>2</sub> + M ↔ 2OH + M) has strong positive sensitivity coefficient. As the concentration of OH increases, the reaction of OH addition to isobutene to form hydroxy radical adducts, which react with O<sub>2</sub> to form acetone becomes more significant. OH abstraction of H from isobutene has, on other hand, a strong negative sensitivity coefficient, because this reaction competes with OH addition to isobutene.

**Reactions Important to Methacrolein Formation.** Methacrolein is formed by three major reaction paths: the first is C=C(C)C addition with O<sub>2</sub> (reaction pathways I of the C=C(C)C + O<sub>2</sub> reaction system of this study). The second is via β-scission (loss of H atom) from the C=C(C)CO· radical which is produced via the allylic isobutenyl radical combination with HO<sub>2</sub>, and the third is from this same C=C(C)CO· radical where it is formed from OH addition with isobutene and further reaction with O<sub>2</sub> (shown in Scheme 4).

Some methacrolein is lost via abstraction of the aldehydic H atom by OH, HO<sub>2</sub>, CC=C and C=C(C)C radicals to form C=C(C)C=O which rapidly decomposes to CC=C + CO. Sensitivity analysis shows the reaction C=C(C)C + HO<sub>2</sub> ↔ C=C(C)CO· + OH has the greatest positive influence on methacrolein formation. The reaction 2HO<sub>2</sub> ↔ H<sub>2</sub>O<sub>2</sub> + O<sub>2</sub> shows the highest negative influence, because it consumes HO<sub>2</sub> radical.

**HO<sub>2</sub> Radical and H<sub>2</sub>O<sub>2</sub>.** The initiation reaction 1 C=C(C)C + O<sub>2</sub> ↔ C=C(C)C + HO<sub>2</sub> provides an initial source of HO<sub>2</sub> radicals; but HO<sub>2</sub> is also formed in the reaction processes of isobutenyl radical with O<sub>2</sub>. As HO<sub>2</sub> radical concentration increases, hydrogen peroxide can be formed by the reaction 2HO<sub>2</sub> ↔ H<sub>2</sub>O<sub>2</sub> + O<sub>2</sub> and by HO<sub>2</sub> abstraction of H atom from isobutene (C=C(C)C + HO<sub>2</sub> ↔ C=C(C)C + H<sub>2</sub>O<sub>2</sub>). As the hydrogen peroxide concentration increases, the reactive OH radical is produced from the thermal decomposition of hydrogen

peroxide (H<sub>2</sub>O<sub>2</sub> + M ↔ 2OH + M). The OH radical also can be formed byproduct formation reactions of C=C(C)C + HO<sub>2</sub> ↔ C=C(C)CO· + OH and C=C(C)C + O<sub>2</sub> ↔ C=C(C)CO· + OH which are the important processes to methacrolein and methylene oxirane formation, respectively. As OH radical concentration increases, the reactions between C=C(C)C and OH (both abstraction and addition reaction) become significant.

Sensitivity analysis shows that an increase in the A factor of reaction C=C(C)C + OH ↔ C=C(C)C + HO<sub>2</sub> by a factor of 2, results in a decrease of acetone (by 27%) and methacrolein (by 18%). Increases are observed for 2,5-dimethylhexa-1,5-diene (by 17%) and methylene oxirane (by 17%) respectively, at 743 K and 60 Torr (reaction time = 180 s). On the other hand, an increase in the A factor of reaction C=C(C)C + OH ↔ C<sub>3</sub>COH by a factor of 2, results in an increase of acetone (by 41%) and methacrolein (by 0.6%) with decreases for 2,5-dimethylhexa-1,5-diene (by 1.4%) and methylene oxirane (by 1.0%), respectively. An increase in the A factor of reaction C=C(C)C + HO<sub>2</sub> ↔ C=C(C)COOH by a factor of 2, results in increases of acetone (by 0.8%) and methacrolein (by 4%); but decreases in 2,5-dimethylhexa-1,5-diene (by 0.5%) and methylene oxirane (by 0.5%), respectively.

**Model and Comparison to Experimental Data.** An elementary reaction mechanism has been developed to model the experimental system, isobutene oxidation. The CHEMKIN II interpreter and integrator, version 3.1, is used to model the reaction conditions of Ingham et al.<sup>7</sup> for reaction time range (0–210 s), 743 K and 60 Torr (mole fractions of isobutene:O<sub>2</sub>:N<sub>2</sub> = 0.067:0.5:0.433). Abstraction reactions are not considered pressure dependent and, therefore, do not require falloff analysis. Abstraction reactions of O, OH, HO<sub>2</sub> and R· radicals are taken from evaluated literature wherever possible. A procedure from Dean and Bozzelli<sup>41</sup> is used to estimate abstraction rate constants by H, O, OH and CH<sub>3</sub> radicals when no literature data are available. A generic rate constant is utilized and adjusted for steric effects and reaction enthalpy for hydrogen abstractions by C=CC· and HO<sub>2</sub> radicals.<sup>42</sup> The reaction mechanism for conditions of 760 Torr pressure and temperature range from 500 to 900 K is available in the Supporting Information.

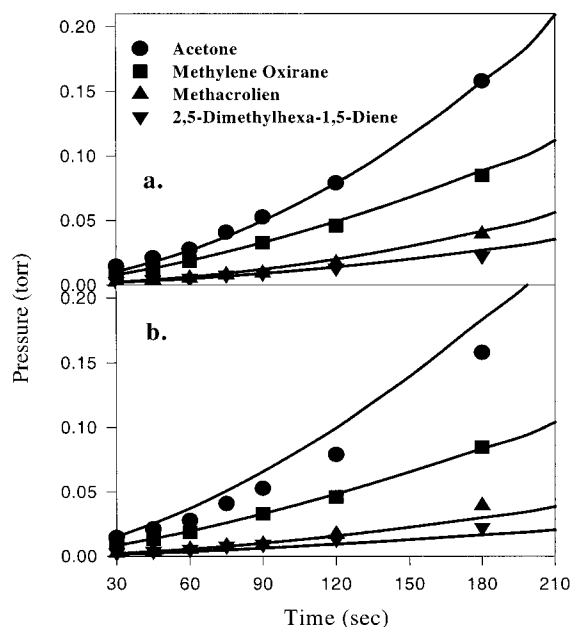


**Figure 4.** Comparison model prediction and experimental data. Symbols are experimental data from Ingham et al.<sup>7</sup> for reaction time range (0–210 s), 743 K and 60 Torr (molar fraction of isobutene:O<sub>2</sub>:N<sub>2</sub> = 0.067:0.5:0.433). Lines are calculations based on thermodynamic parameters from (a) CBS-q//MP2(full)/6-31g(d) and (b) B3LYP/6-311+g(3df,2p)//B3LYP/6-31g(d) levels, respectively.

Figure 4 shows that comparison of our calculation with experimental data for productions of 2,5 dimethylhexa-1,5-diene, methacrolein, isobutene oxides and acetone over the reaction time range (0–210 s), 743 K and 60 Torr. Calculations based on thermodynamic parameters from CBS-q//MP2(full)/6-31g(d) and B3LYP/6-311+g(3df,2p)//B3LYP/6-31g(d) levels are illustrated in Figure 4a and 4b, respectively; and symbols are data of Ingham et al.<sup>7</sup> Calculated isobutene oxides are included 2,2-dimethyloxirane (three-member ring oxirane)(16%) and methylene oxirane(84.5%). 2,2-dimethyloxirane is formed primarily from C<sub>3</sub>•COOH, which is from the HO<sub>2</sub> radical addition to isobutene. HO<sub>2</sub> addition to isobutene to form C<sub>3</sub>•COOH is the important path for oxirane formation and has been thoroughly discussed in our previously study.<sup>38</sup> The results using CBS-q//MP2(full)/6-31g(d) calculation on 2,5-dimethylhexa-1,5-diene, methacrolein, and isobutene oxides product formation are in excellent agreement with experimental data of Ingham et al.<sup>7</sup> Acetone formation is overestimated based on B3LYP/6-311+g(3df,2p)//B3LYP/6-31g(d) calculation, but CBS-q values lead to good agreement.

This isobutene oxidation mechanism is also used to model the experimental conditions of Knyazev et al.<sup>10</sup> for the decay constant of the C<sup>•</sup>–C(C)–C radical at 800K and 2.78 Torr in He bath gas and varied [O<sub>2</sub>]. The pseudo-first-order radical decay constants, *k'*, are calculated at different concentration of O<sub>2</sub>. The radical decay *k'* vs [O<sub>2</sub>] at 800K and 2.78 Torr in He bath gas is available in the Supporting Information. The second-order rate constant of the reaction of C<sup>•</sup>–C(C)–C radical with O<sub>2</sub> is calculated to be 1.06 × 10<sup>7</sup> s<sup>-1</sup> mol<sup>-1</sup> cm<sup>3</sup> and 4.51 × 10<sup>7</sup> s<sup>-1</sup> mole<sup>-1</sup> cm<sup>3</sup> based on thermodynamic parameters from CBS-q//MP2(full)/6-31g(d) and B3LYP/6-311+g(3df,2p)//B3LYP/6-31g(d) calculations, respectively. These small rate constants are consistent with experiment of Knyazev et al., *k* < 10<sup>8</sup> s<sup>-1</sup>mol<sup>-1</sup>cm<sup>3</sup>, where no reaction of the allylic isobutenyl radical with molecule oxygen could be observed at 800 K and 2.78 Torr.

Figure 5a and 5b shows the concentration of reactant (C<sup>•</sup>–C(C)–C) and products vs reaction time based on the CBS-q//MP2(full)/6-31g(d) mechanism at two different O<sub>2</sub> concentrations. OH, HO<sub>2</sub>, H<sub>2</sub>O, O, CO, CO<sub>2</sub>, CH<sub>2</sub>O, ketene (C=C=O), allene (C=C=C), 2,5-dimethylhexa-1,5-diene, methylene oxirane, methacrolein are primary products. Figure 5a shows that the C<sup>•</sup>–C(C)–C undergoes association, reaction 7, to form 2,5-dimethylhexa-1,5-diene and dissociation to C=C=C + CH<sub>3</sub> radical at lower O<sub>2</sub> concentration ([O<sub>2</sub>] = 4.84 × 10<sup>14</sup> molecules/cm<sup>3</sup> at 800 K and 2.78 Torr). Figure 5b shows that the C<sup>•</sup>–C(C)–C reacts with O<sub>2</sub> forming adducts and isomers, which rapidly dissociate (entropy driven) back to reactants showing a low rate constant to products, at high O<sub>2</sub> concentration ([O<sub>2</sub>] = 4.84 × 10<sup>16</sup> molecules/cm<sup>3</sup> at 800 K and 2.78 Torr). The equilibrium concentrations of the adducts (from R• + O<sub>2</sub>) at high [O<sub>2</sub>] lowers the C<sup>•</sup>–C(C)–C concentration and therefore limits C<sup>•</sup>–C(C)–C + C<sup>•</sup>–C(C)–C association to 2,5-dimethylhexa-1,5-diene. OH radical forms from reaction paths I and II. HO<sub>2</sub>, H<sub>2</sub>O and O are formed from further reactions of OH radical. CH<sub>2</sub>O forms from reaction paths IIa and III. CO and CO<sub>2</sub> are from further reactions of CH<sub>2</sub>O. Ketene (C=C=O) forms from C<sup>•</sup>–C(C)–O radical, which is formed from reaction path III. The C<sup>•</sup>–C(C)–O radical undergoes β-scission forming C=C=O and CH<sub>3</sub> radical. Allene (C=C=C) forms from reaction path IIa and via β-scission of C<sup>•</sup>–C(C)–C radical to form C=C=C and CH<sub>3</sub> radical.

**Accuracy of Ab Initio and Density Functional CBS Calculations.** A number of researchers<sup>19,76–87</sup> have performed comparison studies on G2, G2(MP2), CBS-q and density function calculations—overall they report that average deviation among these higher level composite methods are within a few kcal/mol (~1.5–4.2) when using atomization reactions for determination of ΔH<sub>f</sub><sup>o</sup><sub>298</sub>. The use of isodesmic reaction with group balance result in better accuracy for stable species and radicals. These researchers also indicate that MP2 calculations overestimate and density function sometimes significantly underestimate transition state barriers, with MP2 determining tighter transition states in comparison to B3LYP. One method of testing accuracy is the comparison of model data to experiment. We report this comparison and note that the only barrier adjusted to obtain the data fit, is dissociation of C=C(C•)COOH ↔ C=C(C•)CO• + OH ↔ C=Y(CCOC) + OH, where the barrier is slightly reduced (less than 0.5 kcal/mol). We acknowledge that in studies on dimethyl ether<sup>85</sup> and tertiary butyl radicals + O<sub>2</sub><sup>38</sup> adjustments of several, ca. 3 kcal/mol, were needed on one important reaction in each system. There are many reactions in these systems, which are difficult or near impossible to study on an elementary reaction level. The use of ab initio and density functional calculations provides important insights to these reaction processes and provides a systematic and consistent method to formulate mechanisms and for estimation of kinetic parameters in hydrocarbon oxidation.

## Summary

A thermochemical and chemical activation reaction analysis is presented on the important reaction system: allylic isobutenyl radical + O<sub>2</sub>. Thermodynamic properties, reaction paths and elementary reactions are presented with kinetic parameters evaluated versus temperature and pressure. An elementary reaction mechanism has been developed to model the intermediate (pre-ignition) temperature isobutene oxidation. An important new reaction path, C=C(C•)COOH ↔ C=C(C•)CO• + OH ↔ C=Y(CCOC) + OH, for methylene oxirane formation is shown to be more important than C=C(C•)COOH ↔ TS5 ↔



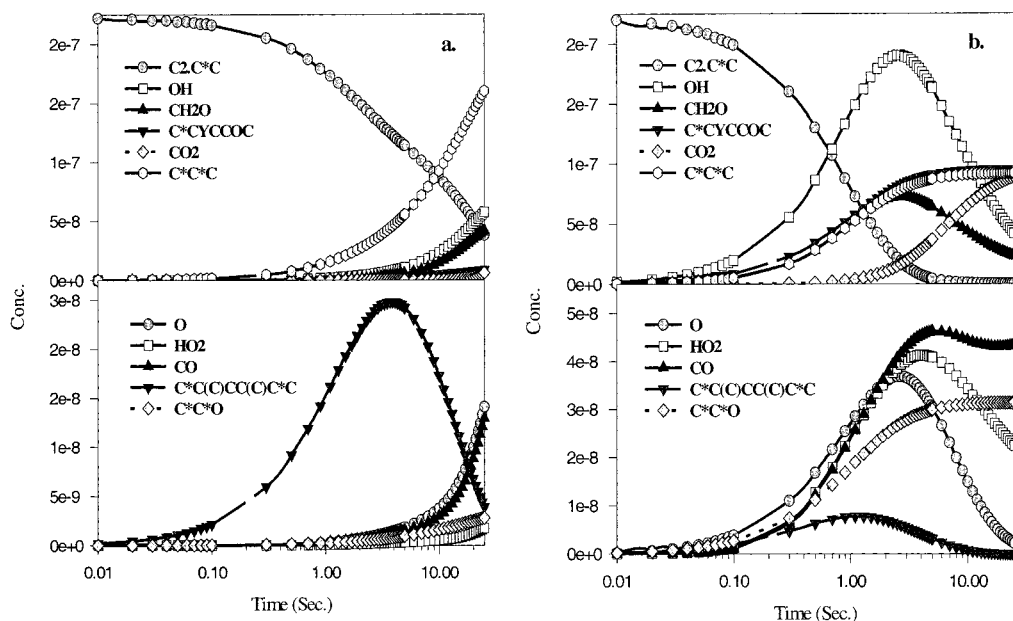


**Figure 5.** Concentration of reactant (C=C(C)CO• radical) and products vs reaction time based on CBS-q/MP2(full)/6-31g(d) mechanism at 800 K, 2.78 Torr in He bath gas and [C=C(C)CO•] =  $2 \times 10^{10}$  molecules cm<sup>-3</sup>. (a) [O<sub>2</sub>] =  $4.84 \times 10^{14}$  molecules cm<sup>-3</sup>; (b) [O<sub>2</sub>] =  $4.84 \times 10^{16}$  molecules cm<sup>-3</sup>.

C=Y(CCOC) + OH at 743 K and 60 Torr for the allylic isobutenyl radical + O<sub>2</sub> reaction. The reaction barrier for the C=C(C)COOH reaction to C=C(C)CO• + OH is evaluated as 42.45 (41.90) kcal/mol with an A factor of  $4 \times 10^{15}$  s<sup>-1</sup>. Reaction barrier of C=C(C)COOH → TS5 → C=YCCOC + OH is calculated as 42.14 kcal/mol with an A factor of  $6.95 \times 10^{11}$  ( $1.03 \times 10^{12}$ ) s<sup>-1</sup> at 743 K. Other calculated barriers are as 28.02 (24.95) and 29.72 (27.98) kcal/mol with A factors of  $4.27 \times 10^{10}$ ,  $2.42 \times 10^{10}$  ( $3.28 \times 10^{10}$ ) and  $3.88 \times 10^{10}$  ( $6.09 \times 10^{10}$ ) s<sup>-1</sup> at 743 K, respectively, for four- and five-member ring cyclization. Results from the mechanism based on CBS-q calculation are in good agreement with experimental data reported by Ingham et al.<sup>7</sup> and by Knyazev et al.<sup>10</sup> The Allylic isobutenyl radical reaction with O<sub>2</sub> forms number of adducts which do not have low energy channels to new products; thus reverse reaction to C=C(C)CO• + O<sub>2</sub> is the dominant adduct dissociation path. High [O<sub>2</sub>] results in lower C=C(C)CO• levels via formation of increased levels (near steady state) of peroxy and peroxide adducts. CBS-q calculations based on MP2(full)/6-31g(d) and B3LYP/6-31g(d) geometries result in reasonable accurate thermodynamic enthalpy data for C=C(C)CO• + O<sub>2</sub> reaction system that agree with results of Jungkamp et al.<sup>16,17</sup> and Petersson et al.<sup>18</sup>

**Acknowledgment.** We are thankful for funding from the US EPA Research Center on Airborne Organics and Dr. Rajiv Berry, the US Airforce Materials Laboratory (MLBT), WPAFB, Ohio, for some computational assistance.

**Supporting Information Available:** Total energies are calculated at MP2 (full)/6-31g(d), B3LYP/6-31g(d), MP4 (full)/6-31g(d, p)//MP2 (full)/6-31g(d), B3LYP/6-31g(d), B3LYP/6-311+g(3df,2p)//B3LYP/6-31g(d) and complete basis set (CBS-4 and CBS-q) model chemistry calculations (Tables S-1 and S-2). The rate constants  $k = AT^n \exp(-E_a/RT)$  for QRRK calculated chemical activation and unimolecular dissociation at pressures of 0.076, 0.76, 7.6, 60, 760, and 7600 Torr and temperature from 300 to 2000K (Table S-3). The reaction mechanism for conditions of 760 Torr pressure and temperature range from

500 to 900 K (Table S-4). The structures, moments of inertia and frequencies for reactant, important intermediates and transition states calculated from MP2(full)/6-31g(d) and B3LYP/6-31g(d) (Table S-5). The radical decay  $k'$  vs [O<sub>2</sub>] at 800 K and 2.78 Torr in He bath gas (Figure S-1). This material is available free of charge via the Internet at <http://pubs.acs.org>.

## References and Notes

- Benassi, R.; Taddie, F. *J. Mol. Struct. (THEOCHEM)* **1994**, *33*, 101.
- Jonsson, M. *J. Phys. Chem.* **1996**, *100*, 6814.
- Bach, R. D.; Ayala, P. Y.; Schlegel, H. B. *J. Am. Chem. Soc.* **1996**, *118*, 12758.
- Raiti, M. J.; Sevilla, M. D. *J. Phys. Chem.* **1999**, *103*, 1619.
- Benassi, R.; Folli, U.; Sbardellati, S.; Taddei, F. *J. Comput. Chem.* **1993**, *4*, 379.
- Brezinsky, K.; Dryer, F. L. *Combust. Sci. Tech.* **1986**, *45*, 225.
- Ingham, T.; Walker, R. W.; Woolford, R. E. *25th Symposium (Intern'l) on Combustion, The Combustion Inst.* **1994**, 783.
- Bauge, J. C.; Battin-Leclerc, F.; Baronnet, F. *Int. J. Chem. Kinet.* **1998**, *30*, 629.
- (a) Gilbert, R. G.; Smith, S. C. *Theory of Unimolecular and Recombination Reactions*; Oxford Press: 1990. (b) Gilbert, R. G.; Smith, S. C.; Jordan, M. J. T. *UNIMOL program suite (calculation of falloff curves for unimolecular and recombination reactions)*; 1993. Available from the authors: School of Chemistry, Sydney University, NSW 2006, Australia or by email to: gilbert\_r@summer.chem.su.oz.au. (c) Personal communication Dean, A. M., Chang, A. Y., Exxon Corp. Res. Annandale NJ. (d) Gilbert, R. G.; Luther, K.; Troe, J. *Ber. Bunsen-Ges. Phys. Chem.* **1983**, *87*, 164.
- Personal communication Knyazev, V. D., The Catholic University of American, Washington, D.C.
- (a) Stewart, J. J. P. *MOPAC 6.0*, Frank J. Seiler Research Lab., US Air Force Academy: Colorado, 1990. (b) PC-Windows 95 version compiled by C. Sheng NJIT.
- Frisch, M. J.; Trucks, G. W.; Head-Gordon, M.; Gill, P. M. W.; Wong, M. W.; Foresman, J. B.; Johnson, B. G.; Schlegel, H. B.; Robb, M. A.; Pople, E. S.; Gomperts, R.; Andres, J. L.; Raghavachari, K.; Binkley, J. S.; Gonzalez, C.; Martin, R. L.; Fox, D. J.; Defrees, D. J.; Baker, J.; Stewart, J. J. P.; Pople, J. A., Eds.; *Gaussian 94 Computer Program, Revision C 2*; Gaussian Inc.: Pittsburgh, 1995.
- Montgomery, J. A.; Ochterski, J. W.; Petersson, G. A. *J. Chem. Phys.* **1994**, *101*, 5900.
- Ochterski, J. W.; Petersson, G. A.; Wiberg, K. B. *J. Am. Chem. Soc.* **1995**, *117*, 11299.
- Ochterski, J. W.; Petersson, G. A.; Montgomery, J. A. *J. Chem. Phys.* **1996**, *104*, 2598.

- (16) Petersson, G. A.; Tensfeldt, T. G.; Montgomery, J. A. *J. Chem. Phys.* **1991**, *94*, 6091.
- (17) Petersson, G. A.; Al-Laham, M. A. *J. Chem. Phys.* **1991**, *94*, 6081.
- (18) Petersson, G. A.; Bennett, A.; Tensfeldt, T. G.; Montgomery, J. A.; Shirley, M. A.; Mantzaris, J. J. *J. Chem. Phys.* **1988**, *89*, 2193.
- (19) Yamada, T.; Lay, T. H.; Bozzelli, J. W. *27th Symposium (Intern'l) on Combustion, The Combustion Inst.* **1998**.
- (20) Scott, A. P.; Radom, L. *J. Phys. Chem.* **1996**, *100*, 16502.
- (21) Pitzer, K. S.; Gwinn, W. D. *J. Chem. Phys.* **1942**, *10*, 428.
- (22) Westmoreland, P. R.; Howard, J. B.; Longwell, J. P.; Dean, A. M. *AIChE Annual Meeting*; 32, 1986, 1971.
- (23) Westmoreland, P. R. *Combust. Sci. and Technol.* **1992**, *82*, 1515.
- (24) Dean, A. M.; Westmoreland, P. R. *Int. J. Chem. Kinet.* **1987**, *19*, 207.
- (25) Steinfeld, J. I.; Franciso, J. S.; Hase, W. L. *Chemical Kinetics and Dynamics*; Prentice Hall, NJ, 1989.
- (26) Ritter, E. R. *J. Chem. Info. Comput. Sci.* **1991**, *31*, 400. Ritter, E. R. *Int. J. Chem. Kinet.* **1997**, *29*, 3, 161.
- (27) Bozzelli J. W.; Chang, A. Y.; Dean, A. M. *Int. J. Chem. Kinet.* **1997**, *29*, 3, 161.
- (28) Hirschfelder, J. O.; Curtiss, C. F.; Bird, R. B. *Molecular Theory of Gases and Liquids*, 2nd ed.; Wiley: London, 1963.
- (29) Reid, R. C.; Prausnitz, J. M.; Sherwood, T. K. *Properties of Gases and Liquids*, 4th ed.; McGraw-Hill: New York, 1987.
- (30) Bozzelli, J. W.; Dean, A. M. *J. Phys. Chem.* **1990**, *94*, 3313.
- (31) Bozzelli, J. W.; Dean, A. M. *J. Phys. Chem.* **1993**, *97*, 4427.
- (32) Douhou, S.; Perrin, D.; Martin, R. *J. Chim. Phys.* **1994**, *91*, 1597.
- (33) Tsang, W. *J. Phys. Chem. Ref. Data* **1991**, *20*, 221.
- (34) Jenkin, M. E.; Murrells, T. P.; Shalliker, S. J.; Hayman, G. D. *J. Chem. Soc., Faraday Trans.* **1993**, *89*, 433.
- (35) Slagle, I. R.; Park, J.-Y.; Heaven, M. C.; Gutman, D. *J. Am. Chem. Soc.* **1984**, *106*, 4356.
- (36) Ruiz, R. P.; Bayes, K. D.; Macpherson, M. T.; Pilling, M. J. *J. Phys. Chem.* **1981**, *85*, 1622.
- (37) Mallard, W. G.; Westley, F.; Herron, J. T.; Hampson, R. F.; Frizzell, D. H. *NIST Chemical Kinetics Database, Version 2Q98*, NIST Standard Reference Data, Gaithersburg, MD, 1998.
- (38) Chen, C. J.; Bozzelli, J. W. *J. Phys. Chem.* **1999**, *103*, 9731.
- (39) Chen, C. J.; Bozzelli, J. W. Reaction Pathways and Kinetic Analysis on Methyl tert-Butyl Ether Pyrolysis and Oxidation Reactions. *Chemical and Physical Processes in Combustion*, Proceedings of Eastern Section Combustion Institute Fall Technical Meeting, 2, pp 37–40, North Carolina State University, Raleigh, NC, October 10–13, 1999.
- (40) Baldwin, R. R.; Walker, R. W.; Langford, D. L. *Trans. Faraday Soc.* **1969**, *65*, 792.
- (41) Dean, A. M.; Bozzelli, J. W. Analysis of Hydrogen Atom Abstraction Reactions *Comb. Chem. Nitro.* **1997**, *1*, 12–15.
- (42) Bozzelli J. W.; Chang, A. Y.; Dean, A. M. *Int. J. Chem. Kinet.* **1997**, *29*, 3, 161.
- (43) Ritter, E. R.; Bozzelli, J. W. *Int. J. Chem. Kinet.* **1991**, *23*, 767.
- (44) Rodgers, A. S. Selected Values for Properties of Chemical Compounds; Thermodynamic Research Center (TRC), Texas A&M University: College Station, TX, 1982.
- (45) Pedley, J. B.; Naylor, R. O.; Kirby, S. P. *Thermodynamic Data of Organic Compounds*; Chapman and Hall: New York, 1986.
- (46) Lay, T. H.; Bozzelli, J. W. *J. Phys. Chem.* **1997**, *101*, 9505.
- (47) Chase, M. W., Jr. *NIST-JANAF Thermochemical Tables, Fourth Edition*; *J. Phys. Chem. Ref. Data*, Monograph 9, **1998**, 1–1951.
- (48) Lay, T. H.; Bozzelli, J. W.; Dean, A. M.; Ritter, E. R. *J. Phys. Chem.* **1995**, *99*, 14514.
- (49) Cohen, N. *J. Phys. Chem. Ref. Data* **1996**, *25*, 6, 1411.
- (50) Baulch, D. L.; Cobos, C. J.; Cox, R. A.; Frank, P.; Hayman, G.; Just, Th.; Kerr, J. A.; Murrells, T.; Pilling, M. J.; Troe, J.; Walker, R. W.; Warnatz, J. *J. Phys. Chem. Ref. Data* **1994**, *23*, 847.
- (51) Baulch, D. L.; Cobos, C. J.; Cox, R. A.; Esser, C.; Frank, P.; Just, Th.; Kerr, J. A.; Pilling, M. J.; Troe, J.; Walker, R. W.; Warnatz, J. *J. Phys. Chem. Ref. Data* **1992**, *21*, 411.
- (52) Lightfoot, P. D.; Roussel, P.; Caralp, F.; Lesclaux, R. *J. Chem. Soc., Faraday Trans.* **1991**, *87*, 3213.
- (53) Kirk, A. D.; Knox, J. H. *Trans. Faraday Soc.* **1960**, *56*, 1296.
- (54) Sahetchian, K. A.; Rigny, R.; Tardieu de Maleissye, J.; Batt, L.; Anwar Khan, M.; Mathews, S. *Symp. Int. Combust. Proc.* **1992**, *24*, 637.
- (55) Mulder, P.; Louw, R. *Recl. Trav. Chim. Pays-Bas* **1984**, *103*, 148.
- (56) Chang, A. Y.; Bozzelli J. W.; Dean, A. M. Submitted to *Int. J. Res. Phys. Chem. Chem. Phys. (Zeitschrift fur Physicalische Chemie)* **2000**.
- (57) Stothard, N. D.; Walker, R. W. *J. Chem. Soc., Faraday Trans.* **1991**, *87*, 241.
- (58) Sengupta, D.; Chandra, A. K. *J. Chem. Phys.* **1994**, *101*, 3906.
- (59) Nguyen, M. T.; Sengupta, D.; Vanquickenborne, L. G. *J. Phys. Chem.* **1996**, *100*, 10956.
- (60) Nguyen, M. T.; Sengupta, D.; Vereecken, L.; Peeters, J.; Vanquickenborne, L. G. *J. Phys. Chem.* **1996**, *100*, 1615.
- (61) Wooldridge, P.; Hanson, R. *25th Symposium (Intern'l) on Combustion, The Combustion Inst.*; Pittsburgh, PA, 1994; p 983.
- (62) Nguyen, M. T.; Sengupta, D. *J. Chem. Phys.* **1997**, *106*, 9703.
- (63) Biggs, P.; Canosa Mas, C. E.; Frachebourg, J. M.; Pan, A.; Shallcross, D. E.; Wayne, R. P. *J. Chem. Soc., Faraday Trans.* **1993**, *89*, 4163.
- (64) Craig, S. L.; Zhong, M.; Choo, B.; Brauman, J. L. *J. Phys. Chem.* **1997**, *101*, 19.
- (65) Zhong, M.; Brauman, J. L. *J. Am. Chem. Soc.* **1996**, *118*, 636.
- (66) Tsang, W. *J. Phys. Chem. Ref. Data* **1990**, *19*, 1–68.
- (67) Tsang, W.; Hampson, R. F. *J. Phys. Chem. Ref. Data* **1986**, *15*, 1087.
- (68) Atkinson, R.; Baulch, D. L.; Cox, R. A.; Hampson, R. F., Jr.; Kerr, J. A.; Rossi, M. J.; Troe, J. *J. Phys. Chem. Ref. Data* **1997**, *26*, 521–1011.
- (69) Herron, J. T. *J. Phys. Chem. Ref. Data* **1988**, *17*, 967.
- (70) Baldwin, R. R.; Walker, R. W. *Symp. Int. Combust. Proc.* **1979**, *17*, 525.
- (71) Tsang, W. *Int. J. Chem. Kinet.* **1973**, *5*, 929.
- (72) Loser, U.; Scherzer, K.; Weber, K. Z. *Phys. Chem. (Leipzig)* **1989**, *270*, 237.
- (73) Alkemade, U.; Homann, K. H. Z. *Phys. Chem. (Neue Folge)* **1989**, *161*, 19–34.
- (74) Ernst, J.; Spindler, K.; Wagner, H. Gg. *Ber. Bunsen-Ges. Phys. Chem.* **1976**, *80*, 645.
- (75) Ambidge, P. F.; Bradley, J. N.; Whytock, D. A. *J. Chem. Soc., Faraday Trans. 1* **1976**, *72*, 1870.
- (76) Curtiss, L. A.; Raghavachari, K.; Redfern, P. C.; Pople, J. A. *J. Chem. Phys.* **1997**, *106*, 1063.
- (77) Durant, J. L. *Chem. Phys. Lett.* **1996**, *256*, 595.
- (78) Durant, J. L.; Rohlfing, C. M. *J. Chem. Phys.* **1993**, *98*, 8031.
- (79) Ochterski, J. W.; Petersson, G. A. *J. Chem. Phys.* **1996**, *104*, 2598.
- (80) Personal communication, Fox, D., Gaussian Inc.
- (81) Personal communication, Petersson, G. A., Wesleyan University, Middletown, Connecticut.
- (82) Jungkamp, T. P. W.; Seinfeld, J. H. *J. Chem. Phys.* **1997**, *107*, 1513.
- (83) Mebel, A. M.; Diau, E. W. G.; Lin, M. C.; Morokuma, K. *J. Am. Chem. Soc.* **1996**, *118*, 9759.
- (84) Jungkamp T. P. W.; Smith J. N.; Seinfeld, J. H. *J. Phys. Chem.* **1997**, *101*, 4392.
- (85) Yamada, T.; Bozzelli, J. W. Kinetic and Thermodynamic Analysis on Dimethyl-ether + O<sub>2</sub> Reaction (Application of ab initio Calculation, CBS-q and G2). *J. Phys. Chem.*, in press.
- (86) Yamada, T.; Bozzelli, J. W. *J. Phys. Chem.* **1999**, *103*, 7646.
- (87) Wang, H.; Brezinsky, K. *J. Phys. Chem.* **1998**, *102*, 1530.
- (88) Troe, J. In *Combustion Chemistry*; Gardiner W. C., Jr., Ed.; Springer-Verlag: New York, 1984.
- (89) Knyazev, V. D. *J. Phys. Chem.* **1996**, *100*, 5318.
- (90) Bozzelli, J. W., unpublished work for n-propyl oxidation.
- (91) Cohen, N.; Westberg, K. R. *J. Phys. Chem. Ref. Data* **1983**, *12*, 531.
- (92) Cohen, N.; Westberg, K. R. *J. Phys. Chem. Ref. Data* **1991**, *20*, 1211–1311.
- (93) Bencsura, A.; Knyazev, V. D.; Slagle, I. R.; Gutman, D.; Tsang, W. *Ber. Bunsen-Ges. Phys. Chem.* **1992**, *96*, 1338–1347.
- (94) Tsang, W. *J. Phys. Chem. Ref. Data* **1988**, *17*, 887.
- (95) Vereecken, L.; Peeters, J. *J. Phys. Chem.* **1999**, *103*, 1768.
- (96) Schwartz, M.; Marshall, P.; Berry, R. J.; Ehlers, C. J.; Petersson, G. A. *J. Phys. Chem.* **1998**, *102*, 10074.
- (97) Louis, F.; Gonzalez, C. A.; Huie, R. E.; Kurylo, M. J. *J. Phys. Chem.* **2000**, *104*, 2931.
- (98) Clifford, E. P.; Wenthold, P. G.; Gareyev, R.; Lineberger, W. C.; DePuy, C. H.; Bierbaum, V. M.; Ellison, G. B. *J. Chem. Phys.* **1998**, *109*, 10293.
- (99) Ignatyev, I. S.; Xie, Y.; Allen, W. D.; Schaefer, H. F., III *J. Chem. Phys.* **1997**, *107*, 141.
- (100) Maranzana, A.; Ghigo, G.; Tonachini, G. *J. Am. Chem. Soc.* **2000**, *122*, 1414–1423.